

Review

# From aggregation-induced emission to organic room temperature phosphorescence through suppression of molecular vibration

Tongyue Wu,<sup>1</sup> Jianbin Huang,<sup>1</sup> and Yun Yan<sup>1,\*</sup>

## SUMMARY

With the rapid development of aggregation-induced emission (AIE), the principles of AIE have also been shown to stimulate the design of organic room temperature phosphorescence (RTP). Without reverting to heavy covalent synthesis, suppression of the molecular vibration of most AIE molecules containing hybrid atoms is a general strategy leading to RTP. The suppression protocols focus on improving the physical environment of the phosphors, which can be achieved by various noncovalent interactions, as well as physical space confinement. In this review, the following processes are summarized: (1) RTP facilitated by classical host-guest interaction; (2) RTP in non-classical host-guest systems; (3) RTP facilitated by polymer network, including the suppression of the vibration via covalent interaction, noncovalent interaction, physical space confinement, or clusterization of the polymer chains; and (4) RTP in small molecules/simple ions. Finally, a perspective is provided to envision future trends in development of RTP.

## INTRODUCTION

Room temperature phosphorescence (RTP) with long lifetime and large Stokes shift has broad applications in fields ranging from biological imaging<sup>1–3</sup> and light-emitting diodes<sup>4–6</sup> to optical switches.<sup>7–9</sup> Compared with the earlier developed inorganic room temperature phosphorescence, organic room temperature phosphorescence (ORTP) can effectively reduce the price and potential toxicity of the materials by avoiding the employment of metals. The fundamental requirement for the generation of ORTP is the sufficiently efficient intersystem crossing<sup>10,11</sup> (ISC) (Scheme 1), which usually occurs when heavy atoms or hybrid atoms are connected to the chromophores to promote the spin-orbit coupling (SOC).<sup>12,13</sup> Furthermore, de-oxygen, suppression of intramolecular rotation/vibration and molecular thermal motion are also required, since the lifetime of ORTP is very long, which provides enough time for the triplet state to be annihilated by these factors.<sup>14,15</sup>

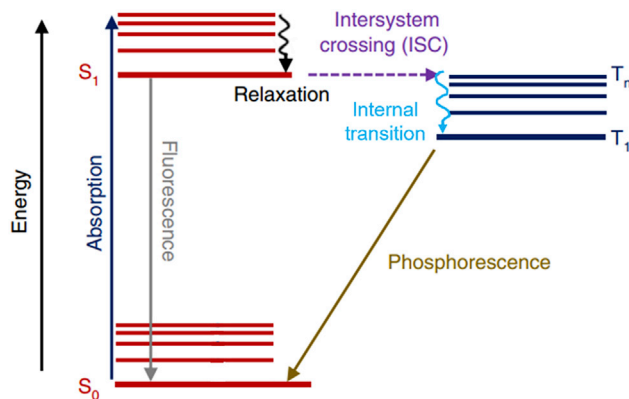
In recent years, inspired by inorganic RTP, crystal engineering of organic chromophores is considered very effective for ORTP.<sup>16</sup> However, the intermolecular π-π stacking in the crystals often leads to the annihilation of triplet-triplet excitons, which dissipates a large number of triplet excitons, thus reducing the phosphorescence efficiency. Due to this limitation, other strategies have been developed.<sup>10</sup> Under this background, ORTP based on aggregation-induced emission (AIE)<sup>17–19</sup> seems very promising since most AIE molecules would form amorphous solids, which naturally avoids the tedious crystal engineering and the low phosphorescence efficiency caused by π-π stacking.

<sup>1</sup>College of Chemistry and Molecular Engineering, Peking University, Beijing 100871, China

\*Correspondence: [yunyan@pku.edu.cn](mailto:yunyan@pku.edu.cn)

<https://doi.org/10.1016/j.xcpr.2022.100771>





**Scheme 1. The electronic transition principles for phosphorescence**

Jablonski diagram illustrating the different photophysical relaxation processes, particularly the intersystem crossing (ISC) between singlet and triplet states, which forms the basis for phosphorescence of organic luminophores.<sup>11</sup>

It has been well known that aggregation-induced emission (AIE) is a phenomenon that the emission becomes stronger or occurs only when the molecules are in aggregated states, including formation of nanoparticles in poor solvent,<sup>20–22</sup> formation of crystals,<sup>23</sup> and simply precipitating in the form of amorphous solids.<sup>24</sup> With the improved understanding on the photo physics behind AIE, it has been recognized that AIE may occur to any propeller or nonplanar luminous molecules if the intramolecular movements, such as rotation and vibration, is prohibited, or if through-space electronic coupling is facilitated. For this reason, a number of subfields have been recognized, such as AIEE (aggregation-induced emission enhancement),<sup>25,26</sup> vibration-induced emission,<sup>27,28</sup> CTE (clusterization-triggered emission<sup>29,30</sup>), and aggregation-induced delayed fluorescence.<sup>31</sup> In many cases, aggregation of the molecules is not necessary for the occurrence of AIE; merely the suppression of the molecular vibration of the AIE molecules is enough to generate the desired emission. As such, host-guest interaction-induced emission,<sup>32,33</sup> interface adsorption-induced emission,<sup>34</sup> and polymer network entrapment-induced emission<sup>35,36</sup> have been reported. Since most AIE molecules contains hybrid atoms, and the restriction of molecular movement is also a necessary requirement for the generation of ORTP, it is envisioned that some AIE systems may also display ORTP. Indeed, ORTPs relevant to AIE have been reported frequently in recent years.<sup>17,18,37</sup>

Lately, there have been quite some excellent review articles on both AIE<sup>38–40</sup> and ORTP.<sup>41–43</sup> However, these reviews generally focus on the individual area of either AIE or ORTP. It is noticed that most ORTP molecules simply display AIE when the molecular vibration and the thermal motion is not prohibited effectively. For this reason, in recent years, many RTPs were created by entrapping AIE molecules via host-guest interactions<sup>44,45</sup> or in a polymeric network.<sup>46,47</sup> Compared with the molecular design strategy that focuses on introducing proper hybrid or heavy atoms to facilitate ISC via SOC,<sup>48,49</sup> the physical strategy of restricting the movement of these molecules seems much more effective in creating RTP, since many of the designed molecules may generate phosphorescence, but not necessarily RTP. Therefore, it is envisioned that a proper strategy of entrapping phosphorous molecules is very crucial to activate their RTP, which is significant toward scaling up fabrication of ORTP materials. With these considerations, this review focuses on noncovalent strategies that awaken the RTP of the AIE molecules containing hybrid atoms. The following contents are included: (1) classical host-guest interaction facilitated RTP,

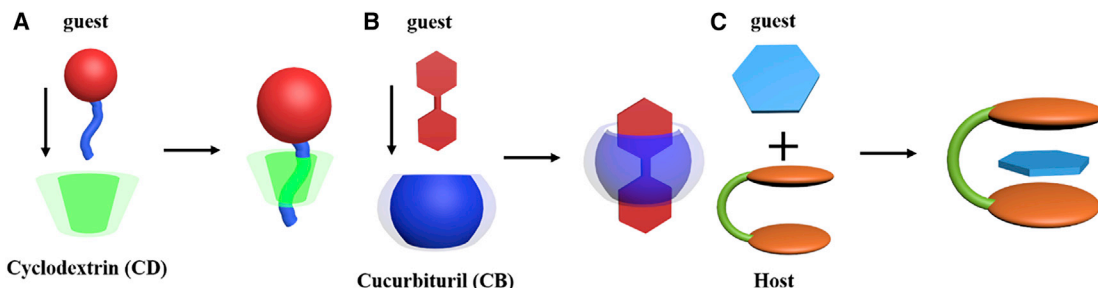


**Figure 1. Types of host-guest interactions**

(A and B) Example of cyclodextrin (A) and cucurbituril (B) based host-guest interaction.  
(C) Host-guest interaction system of non-macrocyclic compounds.

including the host-guest interaction between a phosphor and cyclodextrins (CDs) and cucurbiturils (CBs); (2) RTP enabled in non-classical host-guest systems, where the host either provides a rigid environment for the guest, or specific interaction occurs between the non-macrocyclic host and the guest phosphors; (3) polymer network facilitated RTP, including the suppression of the vibration of the phosphors via covalent interaction, noncovalent interaction, physical space confinement, or clusterization of the polymer chains rich in hybrid atoms; (4) small molecule/simple ion-enabled RTP; and (5) conclusions and perspectives.

## CLASSICAL HOST-GUEST INTERACTION FACILITATED RTP

Host-guest interactions usually refer to the confinement of a molecule by another owing to the specific size or space matching effect.<sup>15,50</sup> Typical host-guest interactions include the threading of a molecule or a particle into the cavity of a cryptate (Figure 1), such as CDs and CBs (Figures 1A and 1B). Sometimes, the imbedding a molecule into the clamp formed by another one may also be called a host-guest interaction (Figure 1C). In recent years, confinement of a molecule into a polymer network or into the arrays formed by other molecules are often named as "host-guest" systems,<sup>51,52</sup> which is not what we referred to as classical "host-guest interactions." In this section, we strictly focus on the classical host-guest interaction facilitated RTP. Macrocyclic compounds such as CDs and CBs with stiff and hydrophobic cavities and stable configuration can create a minimized microenvironment for molecular rotation or vibrational dissipation, which suppress the nonradiative relaxation decay of the excited triplet state, thus greatly enhancing the intensity of phosphorescence.

### CD induced RTP

CDs are the most popular hosts, which are extensively used in supramolecular chemistries.<sup>53–56</sup> CDs are truncated cone-like structures composed of 6, 7, or 8 glucose units, corresponding to  $\alpha$ -cyclodextrin ( $\alpha$ -CD),  $\beta$ -CD, or  $\gamma$ -CD, respectively, linked by 1,4-glycosidic bond. The outer surface of the CDs is hydrophilic owing to the presence of hydroxyl groups, whereas the inner surface is hydrophobic, which is endowed by the ethyl groups.

In 1982, Turro et al. reported the first case of RTP induced by CD (CD-RTP).<sup>57</sup> They observed the phosphorescence of 1-bromonaphthalene and 1-chloronaphthalene in nitrogen-purged aqueous solutions containing  $\beta$ -CD. Through this study, they confirmed that the hydrophobic cavity of CD is strong enough to restrict the vibration of the guest molecules, so that the phosphorescence emission can be achieved even in aqueous solution.

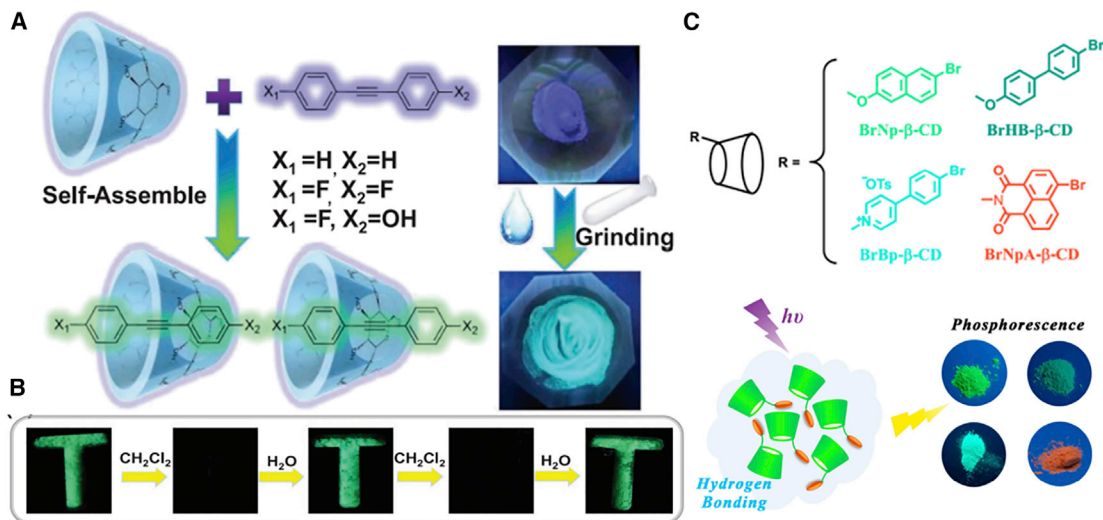


**Figure 2. Cyclodextrins induced RTP**

(A) Schematic diagram of the synthesis of supramolecular complexes.

(B) The photographs of afterglow after cyclically adding dichloromethane and water.<sup>58</sup>

(C) Molecular structures of RTP emissive cyclodextrin derivatives (BrNp- $\beta$ -CD, BrHB- $\beta$ -CD, BrBp- $\beta$ -CD, and BrNpA- $\beta$ -CD) and the resultant RTP amorphous powders under UV irradiation.<sup>59</sup>

Reprinted from Huang and co-workers<sup>58,59</sup> with permissions from John Wiley & Sons (Copyright 2021) and American Chemical Society (Copyright 2018).

Recently, Li and co-workers fabricated a long persistence luminescence (LPL) material from  $\alpha$ -CD and diphenylacetylene (DPA), which makes a further step for CD-based host-guest phosphorescence<sup>58</sup> (Figure 2A). This host-guest complex can self-assemble readily when driven by a trace of water because of the hydrophobic property inside  $\alpha$ -CD. With DPA inside the cavity of  $\alpha$ -CD, a dual color (from green to blue purple) is observed after removing UV irradiation. Interestingly, the LPL of DPA- $\alpha$ -CD supramolecular complex can be turned on and off promptly by spraying water or organic solvent, exhibiting an “LPL switch” property (Figure 2B).

In addition to suppressing the nonradiative relaxation pathway to activate RTP based on the host-guest interaction, the strong intermolecular hydrogen bonding between CDs can also effectively suppress the nonradiative decay processes and shield phosphors from quenchers. In this way, Ma and co-workers modified the phosphor moieties to  $\beta$ -CD, which generates a series of amorphous organic small-molecular compounds displaying RTP from green to orange (Figure 2C).<sup>59</sup> Similar designs were also employed by Liu and co-workers<sup>60</sup> and Yang and co-workers<sup>61</sup> to generate multicolor RTP.

### CB induced RTP

The cucurbit[n]urils (CB[n], n = 6, 7, and 8) are a family of macrocyclic host molecules composed of glycoluril units bridged by methylene groups. However, the geometry of BCs is symmetric drum-like, which renders them enhanced binding strength with guests than CDs. Moreover, the glycoluril moiety in the inner wall is electron-rich, making it able to specifically bind guests with positive charges.<sup>62</sup> For instance, the binding constants for the host-guest systems based on  $\beta$ -CD are usually in the order of  $10^3$ – $10^4$ ,<sup>63</sup> whereas those based on CB[7] can be as high as  $10^7$ – $10^{10}$ .<sup>64</sup> This extremely high binding intensity can immobilize the guests effectively and protect the guests against triplet exciton quenching in solution. For instance, Tao and co-workers for the first time observed the solution-based RTP of quinoline and its derivatives induced by CB[7,8] in 2007.<sup>65</sup> Liu and co-workers reported that CB[6] could

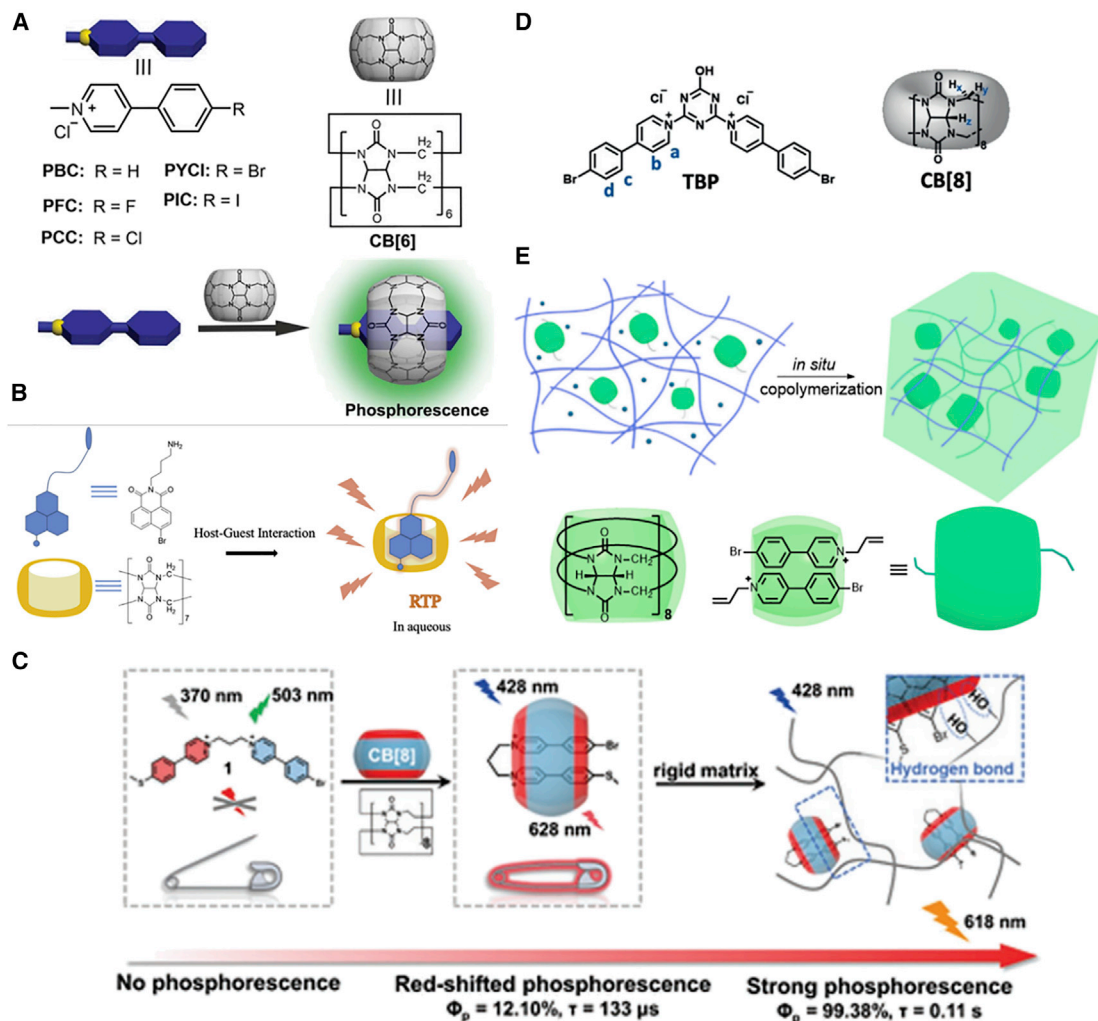


**Figure 3. Cucurbituril induced RTP**

(A) Schematic illustration of the solid-state supramolecular strategy with molecular structure of PYCl and its derivatives.<sup>66,67</sup>

(B) Schematic representation of the CB-RTP system via host-guest interaction between ANBrNpA and CB[7].<sup>68</sup>

(C) Schematic illustration of the formation of supramolecular pin 1/CB[8].<sup>45</sup>

(D) Molecular structure of TBP and CB[8].<sup>69</sup>

(E) Schematic illustration of the construction of the double-network supramolecular hydrogels via *in situ* copolymerization of CB[8]/ABP and acrylamide monomers in the presence of PVA.<sup>70</sup>

Reprinted from Ma and co-workers<sup>45,66,68–70</sup> with permissions from John Wiley & Sons (Copyright 2019, 2021, and 2020) and Elsevier (Copyright 2017 and 2020).

promote the phosphorescence quantum yield of bromophenyl-methyl-pyridinium chloride (PYCl) from 2.6% to 81.2% upon formation of host-guest complex, which is the highest phosphorescence quantum yield of purely organic small-molecule systems so far<sup>66</sup> (Figure 3A). Inspired by this success, this group made a further step to avoid the heavy atoms, which is well known to be effective in facilitating ISC for phosphorescence, generating RTP by immobilizing phosphors into the cavity of CB[6]. They showed that upon removing a heavy atom (Br) from PYCl, an ultralong lifetime of 2.62 s can be obtained<sup>67</sup> (Figure 3A). Since heavy atoms would always result in a shorter lifetime due to the acceleration of radiative and nonradiative decay rates of the triplet state, this CB-based host-guest interaction seems very promising in creating RTP with ultralong lifetimes.

The extent of size matching is very crucial in host-guest interaction facilitated RTP. Since CB[6] has the smallest cavity size, most systems displaying significant phosphorescence enhancement is observed in the host-guest systems based on CB[6]. However, for larger guests, CB[7] and CB[8] can also induce RTP.<sup>69–72</sup> Ma and co-workers reported that 4-bromo-1,8-naphthalic anhydride polymer/CB[7] system is able to emit bright phosphorescence even in aqueous environment<sup>68</sup> (Figure 3B). For larger CB molecules, such as CB[8], the inclusion ratio of host-guest will change from 1:1 into 1:2. Liu and co-workers designed a supramolecular composition of pin 1/CB[8], which displays afterglow with the high phosphorescence quantum yield of 99.38% after incorporation into a rigid matrix. This is the highest yield reported to date for phosphorescent materials<sup>45</sup> (Figure 3C). Similar result can be referred to Ma and co-workers, where by changing the ratio of CB[8] and guest molecules, TBP, a fluorescence-phosphorescence dual-emission and multicolor luminescence can be obtained.<sup>69</sup>

Furthermore, the inclusion ratio of 1:2 for CB[8] and guest molecules provides the possibility for the formation of supramolecular structure<sup>70</sup> (Figure 3D). Ji and co-workers proposed a double-network RTP hydrogel using supramolecular complex (CB[8]/ABP) with commercial polymer polyacrylamide and polyvinyl alcohol (PVA) (Figure 3E). Owning to the double network, this excellent RTP supramolecular hydrogel shows extremely stretchable and tough capability.

### NON-CLASSICAL HOST-GUEST INTERACTION FACILITATED RTP

The fundamental physical insight for the above host-guest interaction-induced RTP is the suppression of the vibration of the guest phosphors in the cavity of CDs and CBs. In fact, except for these typical hosts, other molecules that can effectively suppress the vibration of the phosphors can all serve as the host for corresponding phosphors to generate RTP. We would term them as non-classical host-guest systems. In the non-classical host-guest systems, the host molecules may not only provide a rigid space for the guest, but also be involved in the RTP process through electronic effects, such as charge transfer (CT) or separation, electron donating, pulling, etc. The separation and recombination of charges is the most possible way to achieve ultralong luminescence lifetime comparable with inorganic materials. In addition, the host can also act as an energy donor in fluorescence or phosphorescence resonance energy transfer (FRET/PRET) with guest molecules to achieve high efficiency and multicolor luminescence.<sup>73</sup>

### Hosts serve as non-interacting rigid environments for RTP

The main role of the CDs and CBs in inducing RTP is the suppression of the nonradiative deactivation of the triplet excitons of the guests and shielding them from quenchers. Such a role can also be accomplished by rigid host molecules, which do not have the ring structure but are able to form a stiff complex with the phosphorous guest. Adachi and co-workers<sup>74</sup> reported that structural stiffening can narrow the triplet energy gap difference between host and guest molecules.

Steroidal compounds are a family of such rigid hosts. Adachi and co-workers chose a steroid as the host and the highly deuterated aromatic hydrocarbon as the guest to minimize nonradiative deactivation<sup>75</sup> (Figure 4A). A red-green-blue persistent RTP with a lifetime >1 s and a quantum yield >10% in air was obtained. This material was further used in time-dependent reversible thermal recording media.<sup>76</sup> Estradiols have similar rigid structure to steriodals. Hirata and Vacha utilized β-estradiol

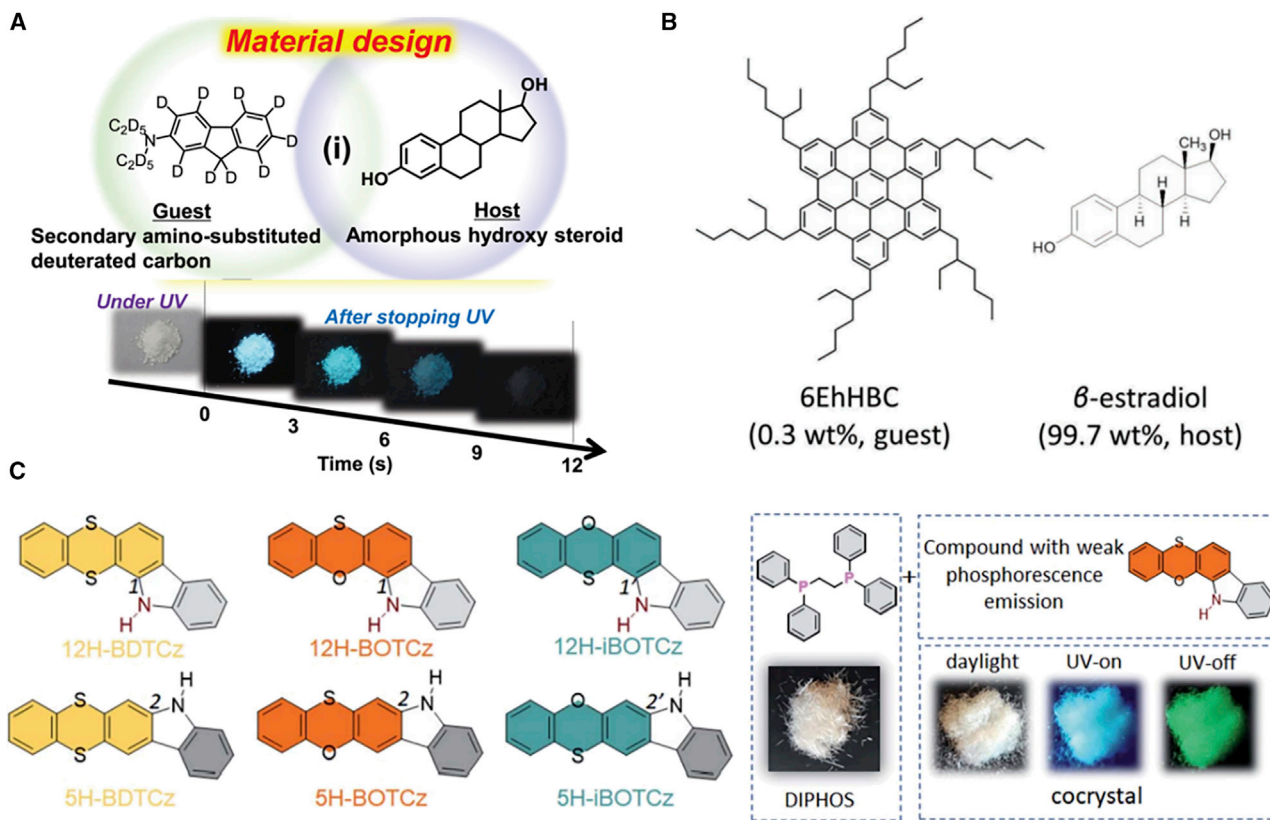


**Figure 4. Rigid environments facilitate RTP**

(A) Molecular structures of deuterated guest and rigid host.<sup>75</sup>

(B) Molecular structure of 2,5,8,11,14,17-hexa(4-(2-ethylhexyl)-hexa-peri-hexabenzocoronene) (6EhHBC) (guest) and  $\beta$ -estradiol (host).<sup>44</sup>

(C) Molecular structures of the host (1,2-bis(diphenylphosphino)ethane [DIPHOS]) and guest molecules.<sup>77</sup>

Reprinted from Hirata and co-workers<sup>44,75</sup> with permissions from John Wiley & Sons (Copyright 2013 and 2017).

as the host and 2,5,8,11,14,17-hexa(4-(2-ethylhexyl)-hexa-peri-hexabenzocoronene) as the guest to create a white RTP<sup>44</sup> (Figure 4B).

In addition to rigid sterol and estradiol, other molecules with aromatic groups may also serve as rigid hosts. For instance, upon employment of 1,2-bis(diphenylphosphino)ethane as the rigid host, it is possible to induce noteworthy RTP enhancement for six weakly phosphorous guests<sup>77</sup> (Figure 4C). In this case, the external heavy-atom effect has promoted the ISC process, and the host-guest interaction has suppressed the aggregation-caused quenching (ACQ) of the emitters.

#### CT between the host and guest induced RTP

LPL is one of the RTPs with a long lifetime. Usually, LPL occurs easily in inorganic materials. Recently, LPL is also realized in organic systems facilitated by a charge-transferring effect. By analyzing three donor materials having similar molecular structures but different energy levels, Adachi and co-workers pointed out the energy gap between the CT and locally excited states is crucial for the design of organic LPL.<sup>78</sup> They found that, when the energy level of the lowest localized triplet excited state is much lower than that of the CT excited state, the system exhibits a short LPL duration and two distinct emissions originating from exciplex fluorescence and donor phosphorescence (Figure 5). However, as this energy gap is large, it generates a higher  ${}^3LE_D$  (the lowest triplet excited state of the donor) population through ISC and

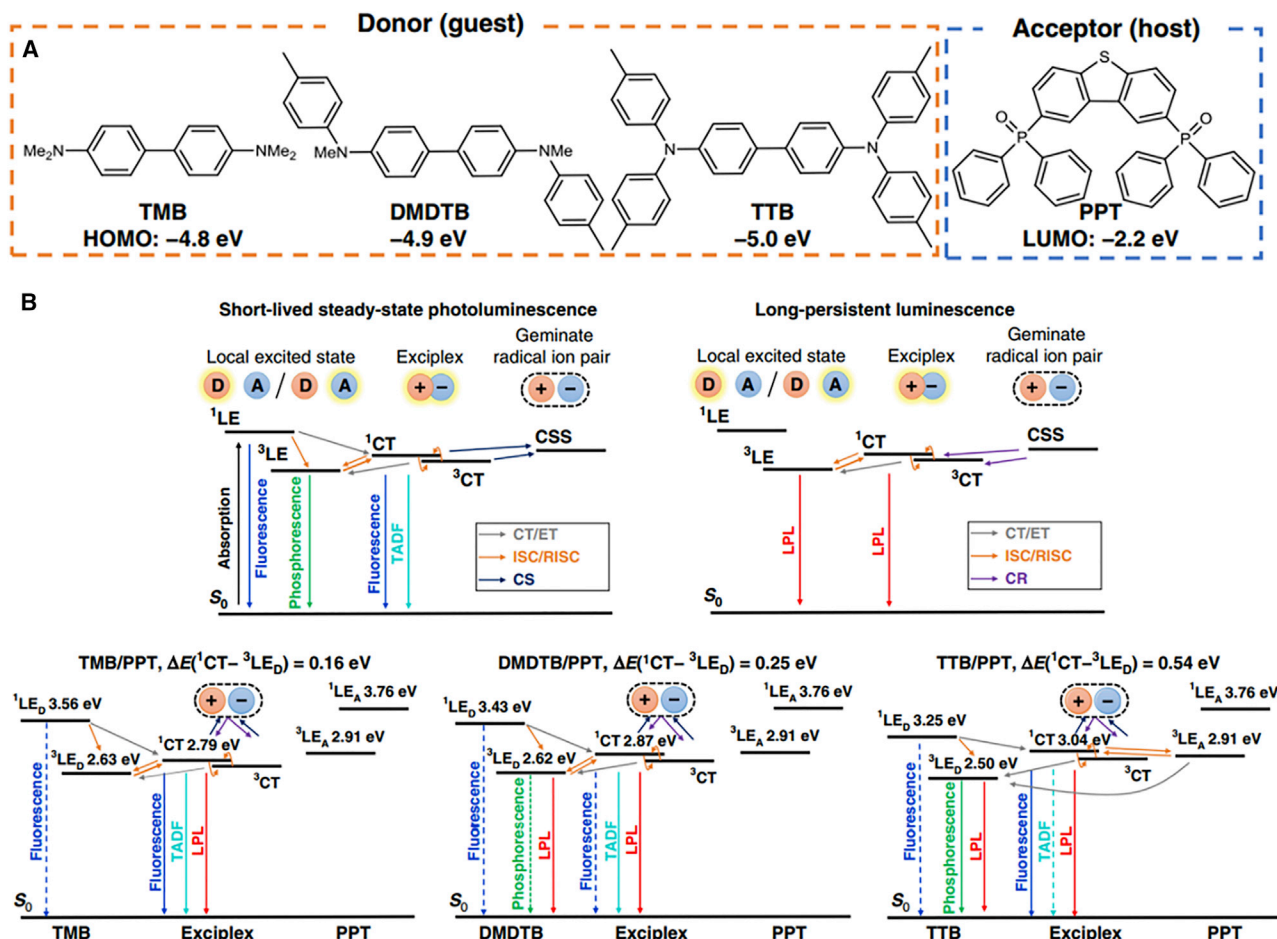


**Figure 5. Charge transfer between the host and guest**

(A) Chemical structures and HOMO or LUMO energy levels of the three electron donors (TMB, DMDTB, and TTB) and the electron acceptor (PPT). (B) Proposed emission mechanism of the OLPL systems.<sup>78</sup>

energy transfer from  ${}^3\text{CT}$  (the lowest singlet excited state of the exciplex) to  ${}^3\text{LE}_D$ , and the emission from both  ${}^1\text{CT}$  and  ${}^3\text{LE}_D$  contribute to LPL. In addition, they found that, even in the absence of an external electric field, some excitons will still undergo exciton dissociation through spontaneous orientation polarization in solid-state films, which provides more possibilities for the design of LPL.<sup>79</sup>

#### Intermolecular D-A interaction induced RTP

Different from the complete CT between the host and the guest, electron donating and accepting may also generate RTP. Dong and co-workers reported that a host-guest co-crystal with electron-donating (D) and electron-accepting (A) molecules can offer another way of forming a CT state for LPL.<sup>80</sup> In this work, they demonstrated a new guest molecule 4-(2-(4-(diphenylamino)phenyl)-2-oxoethyl)benzonitrile (DOB) (Figure 6) with a donor moiety (triphenylamine [TPA]) and an acceptor moiety (benzonitrile). Two precursors of DOB (TPA and 4-(cyanomethyl) benzonitrile [CBN]) are chosen as the donor host and the acceptor guest, respectively. Both donor (TPA) host and acceptor (CBN) guest show weak fluorescence and non-phosphorescence at room temperature. However, after doping into DOB, a significant increase in fluorescence and long-lived persistent luminescence can be easily detected due to the

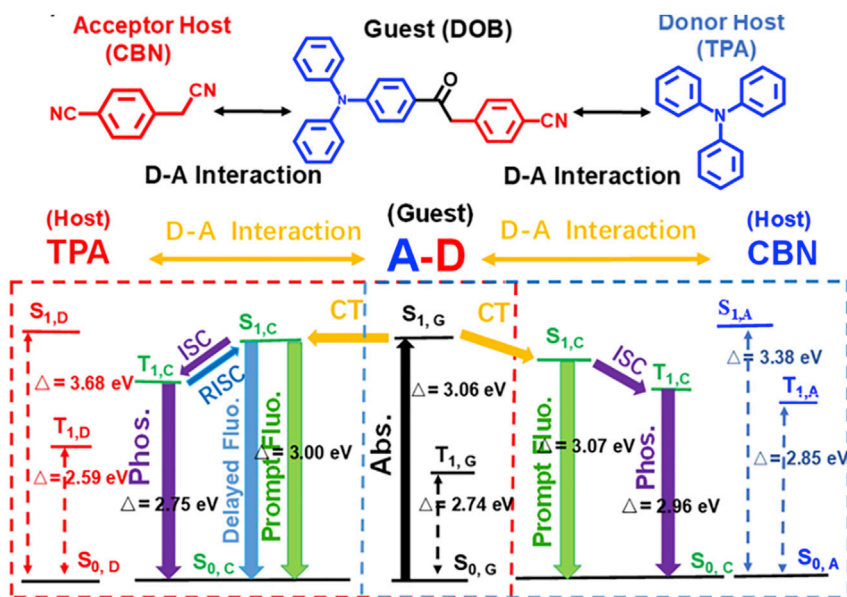


**Figure 6. Intermolecular D-A interaction**

Molecular structure of D-A type host-guest system and its proposed mechanism.<sup>80</sup>  
Reprinted from Li and co-workers<sup>59,80</sup> with permissions from American Chemical Society (Copyright 2019).

intermolecular D-A interaction. This result provides an easy processing way for the development of new charge separation type LPL.

#### RTP host and RTP guest interaction facilitated LPL

Pursuit on both the long lifetime and high phosphorescence yield is the eternal goal in RTP study, since they offer promising opportunities in fields ranging from excitation-free bioimaging to luminescence. Inspired by the molecular stiffening facilitated RTP, Li and co-workers proposed to create the LPL materials with the hosts and guests that both display considerable RTP. To achieve this goal, phenothiazine derivatives were chosen as the guest of the doping system, and their corresponding oxidation products as the host.<sup>81</sup> Since both the host and the guest already display RTP owing to their rigid structure, their crystallization to a much stiffer structure, so that the RTP lifetime can be over 20 min, which is very promising for the application in high-contrast labeling imaging. Owing to the extremely long phosphorescence lifetime, the luminescence signal can be easily captured without real-time light excitation in the subsequent *in vivo* phosphorescence imaging. This is the first *in vivo* phosphorescence imaging report without real-time excitation.

#### Impurities facilitated RTP

Sometimes a minority of guests, just like impurities in the host systems, may generate unexpected RTP, which is especially true for the RTP phenomena observed for some commercialized or newly synthesized small molecules. It has been disclosed that the impurity is the origin of this kind of RTP.<sup>82</sup> This unique impurity-induced phosphorescence phenomenon provides a new design idea for the preparation of phosphorescent materials. Zhang and co-workers discovered that 5-bromo-2-(3,4-dimethoxybenzyl)isoindoline-1,3-dione (BrBID) appeared to possess unusual solvent-dependent RTP.<sup>83</sup> Detailed analysis confirmed that a side reaction with the solvent DMF (byproduct, X) is the main reason for the strong RTP (Figure 7A).

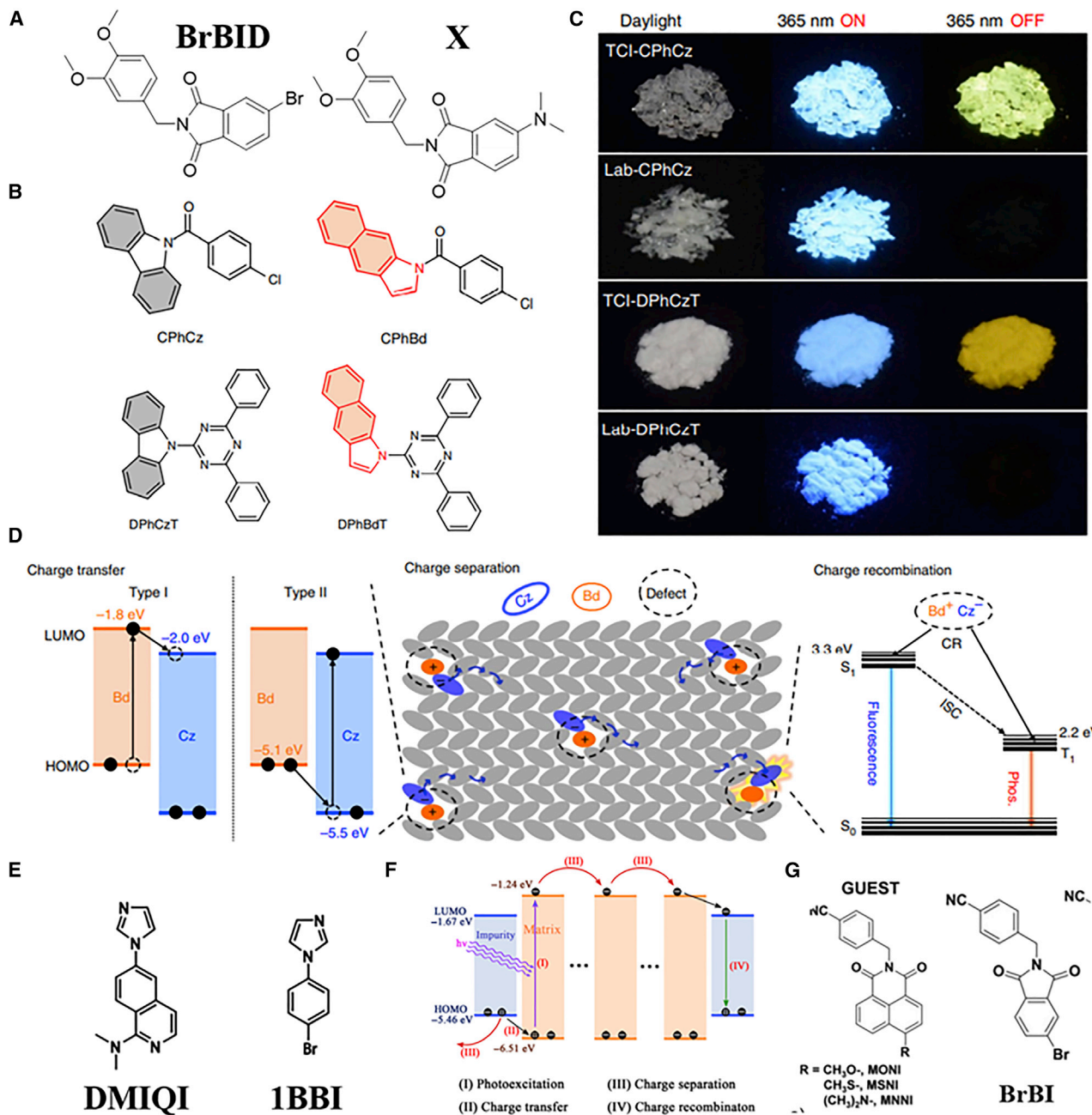


**Figure 7. Impurity-induced RTP**

(A) Chemical structures of BrBID and the byproduct X.<sup>83</sup>

(B) Chemical structures of CPhCz, CPhBd, DPhCzT, and DPhBdT.

(C) Photographs of CPhCz and DPhCzT crystalline powders in daylight and under 365 nm irradiation ON/OFF synthesized from commercially available and lab-synthesized raw materials.

(D) Proposed mechanism of ultralong phosphorescence originated from charge separation.<sup>84</sup>

(E) Chemical structures of 6-(1H-imidazol-1-yl)-N,N-dimethyl isoquinolin-1-amine (DMIQI) and 1-(4-bromophenyl)-1H-imidazole (1BBI).

(F) Proposed mechanism for impurities induced RTP.<sup>85</sup>

(G) Chemical structures of MONI, MSNI, MNNI, and BrBI.<sup>86</sup>

Reprinted from Chen and co-workers<sup>83,84,86</sup> with permissions from John Wiley & Sons (Copyright 2020 and 2021) and Springer Nature (Copyright 2020).

Strikingly, the intense RTP of X was only activated by BrBID matrix through specific molecular orbital interactions.

Although the existence of impurities and their impact on some organic RTP systems was discovered quite early,<sup>87,88</sup> the chemical structure and the impact mechanism of impurities were not specified because of the difficulties in separation, purification, and structural characterization. In their study of the origin of the RTP of the synthesized carbazole, Liu and co-workers for the first time clearly identified each of the impurities in the system and their roles in the RTP<sup>84</sup> (Figures 7B and 7C). Through careful experimental analysis, it is believed that the different electron-donating ability between carbazole isomers helps the formation of a heterojunction-like structure, resulting in the photoinduced charge separation state. It is confirmed that the generation of this charge separation structure plays a vital role in the emergence of ultra-long phosphorescence (Figure 7D).

Coincidentally, Ma and co-workers also observed a trace-impurity-induced 6-(1H-imidazol-1-yl)-N,N-dimethyl isoquinolin-1-amine, with an unusual yellow-green persistent luminescence of 1-(4-bromophenyl)-1H-imidazole powder at room temperature<sup>85</sup> (Figure 7E). The existence of impurities and their impacts on RTP inspired them to design a highly efficient trace-ingredient-mediated bicomponent RTP. A series of artificially added active ingredients were screened out, working as impurities to engender pure organic RTP. This biocomponent RTP can achieve an extra-high quantum yield of up to 74.2% with lifetimes varying from 2 to 430 ms, even with content of impurities lower than 0.1%. The CT between the host and guest and the charge separation-recombination in the impurities play an important role in the enhancement of RTP (Figure 7F).

Deliberate introduction of impurities into a single-component system helps to further understand the mechanism of impurity facilitated RTP. For example, Zhang and co-workers successfully converted the strong fluorescent molecules (MONI, MSNI, and MNNI in Figure 7G) into ultralong RTP by taking them as impurities in the tailored host BrBI.<sup>86</sup> It is noted that the content of the impurities is less than 10 parts per billion. An efficient triplet-triplet energy transfer (TTET) between the delocalized host aggregates and the guest impurities is considered the origin for this impurity-induced RTP.

#### FRET facilitated RTP

Host molecules cannot only play a vital role in providing a rigid environment to suppress nonradiative decay of the guest as mentioned above but also show a synergistic effect to the guest through FRET. Due to the large absorption cross-section of the host molecules, the excitation light absorption efficiency can be maximized, leading to more effective excitation of phosphorescent molecules through energy transfer. Tang and co-workers construct such an energy transfer host-guest system with the commercially available TPB (N,N,N',N'-tetraphenylbenzidine) guest and TPP (triphenylphosphine) or TPA hosts (Figure 8).<sup>89</sup> Both TPB and TPA display fluorescence merely on their own. However, upon formation of a host-guest co-crystal considerable phosphorescence is obtained. The experimental results and theoretical simulation together indicate that: (1) the host molecules not only play a vital role in avoiding quenching of the triplet excited states by oxygen but also restrain the non-radiation transitions to advance the light-emitting efficiency; (2) the host and the guest molecules work synergistically in the photoexcited electronic transition processes. The combination of the two effects generated a greater distinction of  $\emptyset_{ET}$  (energy transfer efficiency), which reveals the occurrence of a complete FRET process in TPB/TPA

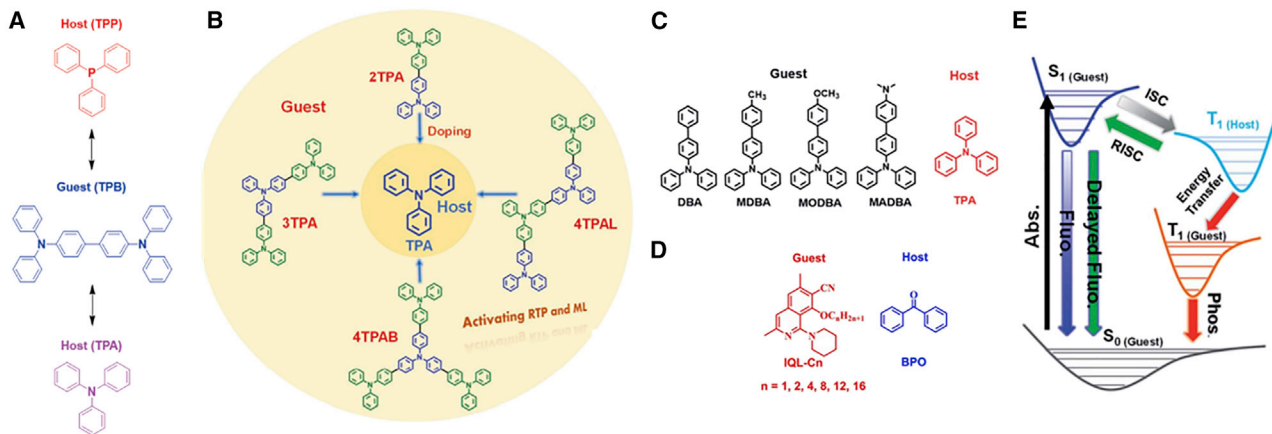


**Figure 8. FRET facilitated RTP**

(A) The chemical structures of host and guest molecules.<sup>89</sup>

(B–D) Molecular design for different host-guest system.<sup>91–93</sup>

(E) Proposed transfer path between the guest and host.<sup>92</sup>

Reprinted from Ning and co-workers<sup>89,91,93</sup> with permissions from Springer Nature (Copyright 2021) and John Wiley & Sons (Copyright 2021 and 2020).

co-crystals, so that no emission originating from TPP appeared in the phosphorescence spectrum. In contrast, TPB/TPP co-crystals underwent an incomplete FRET process following an efficient ISC from the singlet state of TPP to triplet states, thus causing the extra shoulder peak at 458 nm originating from the phosphorescence of TPP (Figures 8B and 8C). In this case, energy level matching, appropriate energy level gap, and sufficiently close distance between the host and the guest are the most important conditions for the energy transfer. A similar host-guest-based FRET system was reported by Li and co-workers as well, where the phosphorescence intensity increases with increasing temperature.<sup>90</sup>

TPA is a commonly used host molecule in RTP systems. With TPA as the energy donor host and TPA derivatives as the energy acceptor guest, Dong and co-workers designed a series of host-guest materials with long lifetime phosphorescence<sup>91,92</sup> (Figures 8B and 8C). Similar results can be obtained in other host-guest-type energy transfer systems.<sup>93,94</sup> For instance, as benzophenone is used as the host, while a series of isoquinoline derivatives with different alkoxy chains are selected as the guests, the emission color of fluorescence and phosphorescence changed simultaneously with varying the alkoxy chain lengths of the guests<sup>93</sup> (Figure 8D). In all these cases, energy transfer between host and guest plays an important role<sup>92</sup> (Figure 8E).

### PRET enabled RTP

Similar to FRET, where the resonance energy transfer starts from a fluorescent energy donor, the resonance energy transfer occurs as well from a phosphorescent energy donor, which leads to PRET. Since the PRET process involves transferring the long-life RTP to a luminescent energy acceptor, the resultant resonance luminescence also features long lifetime like the RTP. Gao and Yan reported the first case of a PRET system in a two-dimensional (2D) layered host-guest system.<sup>95</sup> They pointed out that the intermolecular dipole orientation plays an important role in the efficiency of energy transfer. Using graphene-like layered double hydroxide as the 2D host, while the dicarboxylic benzene as the donor, and the commercial dye, Eosin Y, as the acceptor, an energy transfer efficiency as high as 99.7% can be detected (Figure 9), due to the large overlaps between the emission of the host molecules and the absorption of the guest.

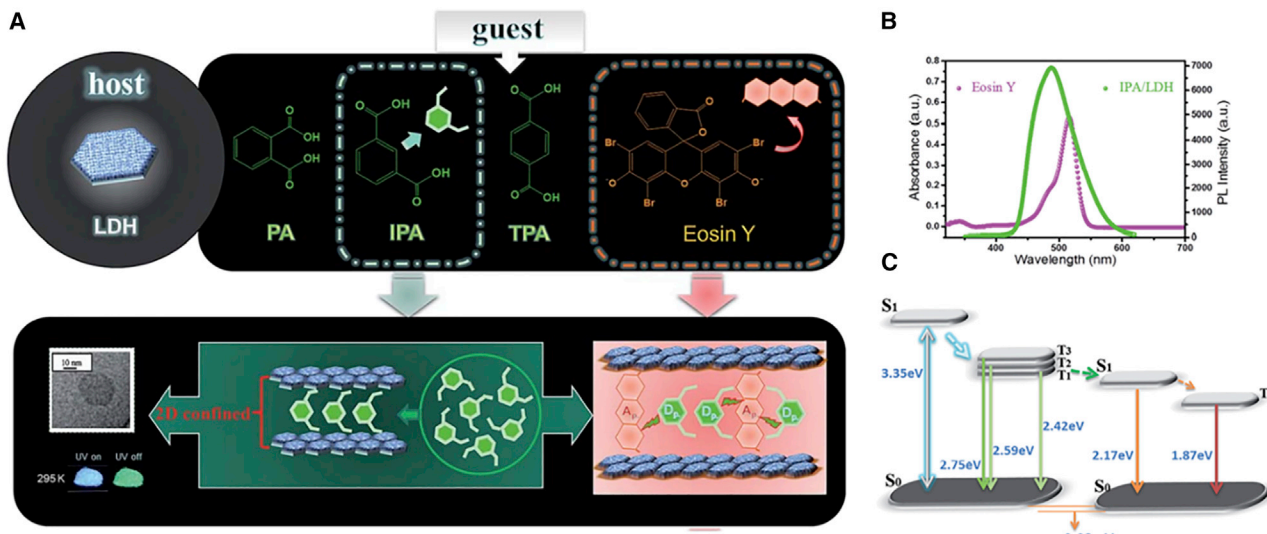


**Figure 9. PRET facilitated RTP**

(A) Schematic representation of the layered double hydroxide (LDH) host and donor/acceptor guest species.  
(B) UV-vis absorption spectrum of pure Eosin Y and phosphorescence spectrum of IPA/LDH.  
(C) Energy levels of states involved in the PET process for (IPA@Eosin Y)/LDH.<sup>95</sup>

In an elegant example reported by Liu and co-workers, the phosphor 4-(4-bromo-phenyl)-pyridine was modified to  $\beta$ -CD (CD-PY).<sup>60</sup> Upon threading into the phosphor into the cavity of CB[8] at a molar ratio of 2:1, a green RTP at 510 nm is generated in solution. With this blue RTP being the energy donor and Rhodamine B (RhB) as the energy acceptor, which form a host-guest complex with the CD moiety of CD-PY, efficient light-harvesting with highly efficient energy transfer and an ultrahigh antenna effect (36.42) occurs through PRET. Importantly, upon assembling the CD-PY@CB[8]@RhB with adamantane-modified hyaluronic acid, which is a cancer cell-targeting agent, into nanoparticles, a further enhanced delayed emission occurred at 590 nm (Figure 10A). A549 cancer cell-imaging experiments indicated that the nanoparticles could be targeted at mitochondria, rendering potential application in delayed fluorescence cell imaging.

In another example from this group,<sup>96</sup> an ultrahigh supramolecular cascaded phosphorescence-capturing aggregate was constructed by multivalent co-assembly of cucurbit[7]uril (CB[7]) and amphiphatic sulfonatocalix[4]arene (SC4AD) (Figure 10B). The initial dibromophthalimide derivative (G) generated a weak phosphorescent emission at 505 nm by host-guest interaction with CB[7], which further assembled with SC4AD to form homogeneously spherical nanoparticles with a dramatic enhancement of both phosphorescence lifetime and emission intensity. Next, this G  $\subset$  CB[7]@SC4AD aggregate is able to exhibit efficient PRET to commercial dye RhB and benzothiadiazole with high efficiency of 84.4% and 76.3% and an antenna effect of 289.4 and 119.5, respectively. This PRET system shows a cascaded energy transfer into near-IR acceptors Cy5 or Nile blue. This delicate host-guest interaction design finally resulted in long-range RTP from 425 to 800 nm. The long-lived photoluminescence was further employed as an imaging agent for multicolor cell labeling.

Like an ordinary FRET system, the energy levels between the host and guest molecules in the phosphorescent systems can be manipulated by finding a proper host for the guest, or vice versa. For instance, upon careful selecting the hosts for the phosphorous guest PzPh, Huang and co-workers accurately adjusted the energy level gap

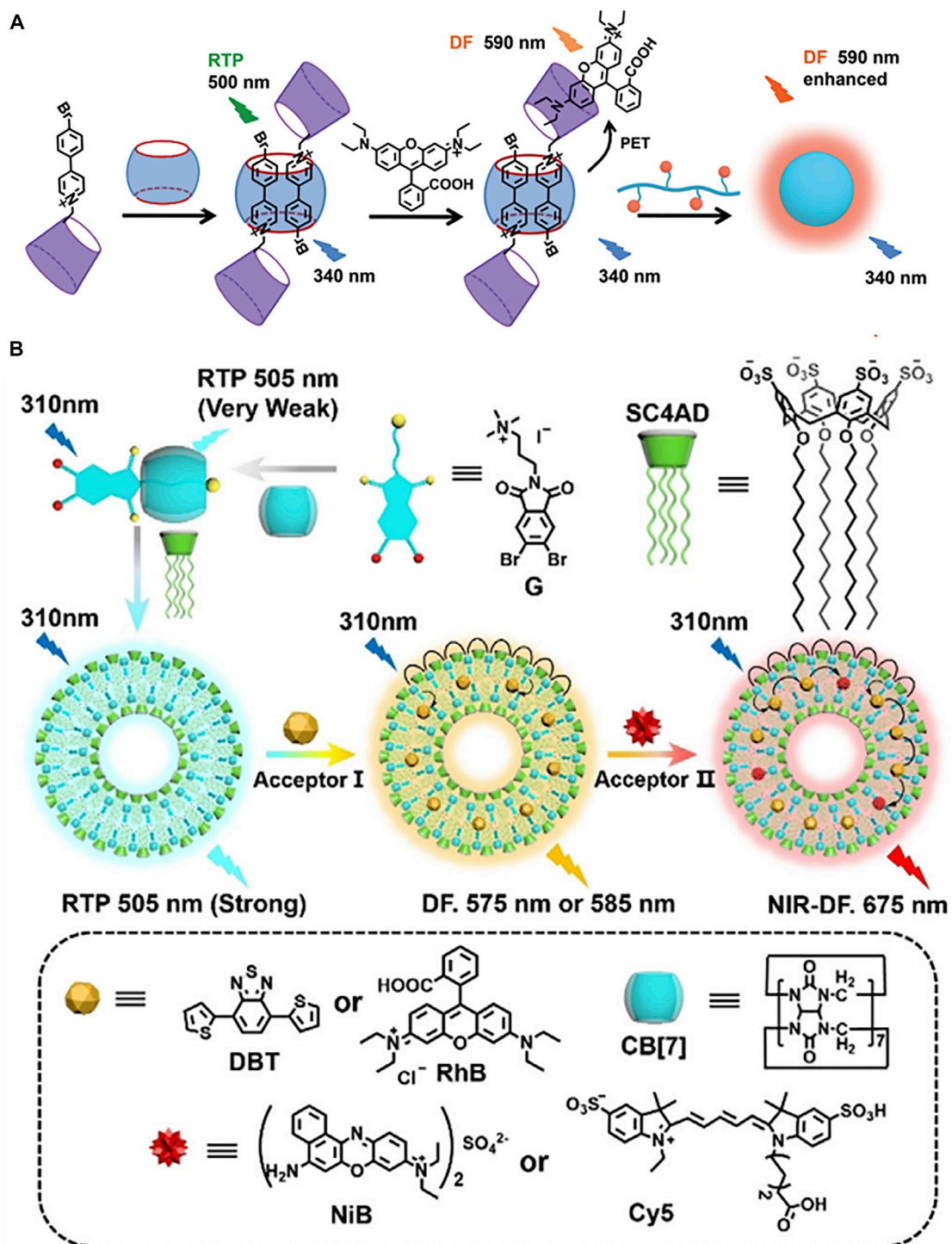


**Figure 10. PRET facilitated RTP with host-guest interactions**

(A) Construction of the supramolecular assembly for a purely organic light-harvesting PET system and related molecules.<sup>40</sup>

(B) Construction of the multivalent supramolecular aggregate for cascaded purely organic room temperature phosphorescence capturing with delayed NIR emission in aqueous solution through highly efficient phosphorescent energy transfer.<sup>96</sup>

Reprinted from Huo et al.<sup>96</sup> with permissions from John Wiley & Sons (Copyright 2021).

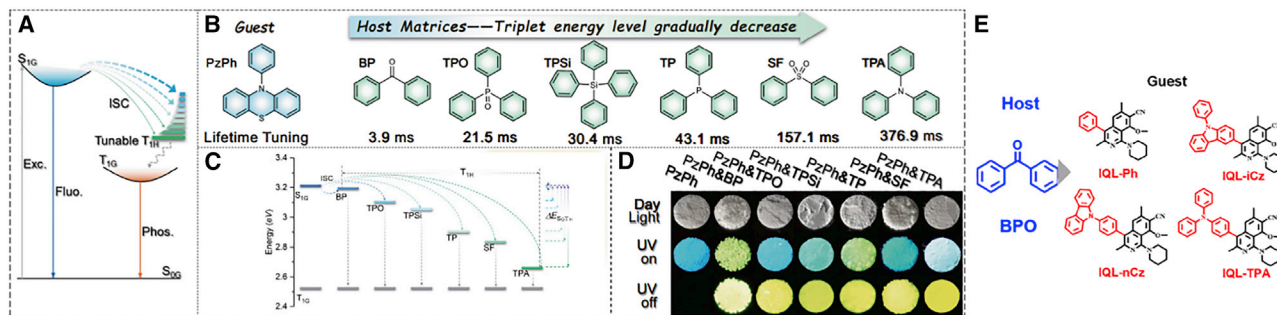


**Figure 11.** RTP with adjustable energy level

(A) Jablonski diagram for ISC and energy transfer pathways between host and guest species.

(B and C) Chemical structures of the guest emitter PzPh and host matrices (BP, TPO, TPSI, TP, SF, and TPA) (B) and their corresponding energy gaps (C).

(D) Photographs of different host-guest combinations.<sup>97</sup>

(E) Molecular structure of host and AIE-guest.<sup>98</sup>

Reprinted from Wang et al.<sup>98</sup> with permissions from American Chemical Society (Copyright 2021).

between host and guest, so that the lifetime varies from 3.9 to 376.9 ms, as large as two orders of magnitude<sup>97</sup> (Figures 11A–11D).

The benefit of the RTP based on PRET is to create excitation wavelength-dependent luminescence, which is especially true in case of the presence of multiple energy transfer paths between the host and the guest molecules. Cai and co-workers achieved this goal by choosing benzophenone as the host and four AIE-active isoquinoline derivatives as the guests (Figure 11E).<sup>98</sup> The host-guest systems exhibited excellent dual-emission characteristics with cyan fluorescence and orange-yellow RTP. The relative intensity of the fluorescence-phosphorescence could be adjusted by changing the excitation wavelength, with the phosphorescence intensity being higher than that of fluorescence under shorter excitation wavelengths and vice versa. This phenomenon can be explained by different energy transfer paths for excitons under different excitation wavelengths.

If two or more small molecules are added into the polymer matrix simultaneously, complex luminescence can be realized; especially when the resonance energy transfer conditions are met, longer wavelength with higher luminescence efficiency becomes possible. For example, Kuila and George chose PVA as the polymer substrate and CS as the small-molecular energy donor (Figure 12), and a multicolor polymeric phosphorescent material was obtained with the help of triplet-to-singlet Förster resonance energy transfer between the donor and the different acceptor chromophores.<sup>99</sup> When the combination of small molecules is reasonable, it is also expected to obtain composite phosphorescent colors, such as ultralong white phosphorescence.<sup>100</sup>

Since PRET has been verified to be a powerful strategy in generating luminescence with long lifetimes, it is an ideal method for afterglow imaging. To this goal, Li and co-workers designed a probe composed of RTP molecule (mTPA) as the phosphorescent generator and a near-infrared (NIR) fluorescent dye as the energy acceptor. Through PRET, they ultimately obtained a redshifted phosphorescent emission at 780 nm, which exhibited excellent afterglow imaging ability in rat.<sup>101</sup>

### POLYMER NETWORK FACILITATED RTP

With the increased understanding on the principles of ORTP, much simpler strategies leading to RTP has been conceived. For instance, many polymers are found

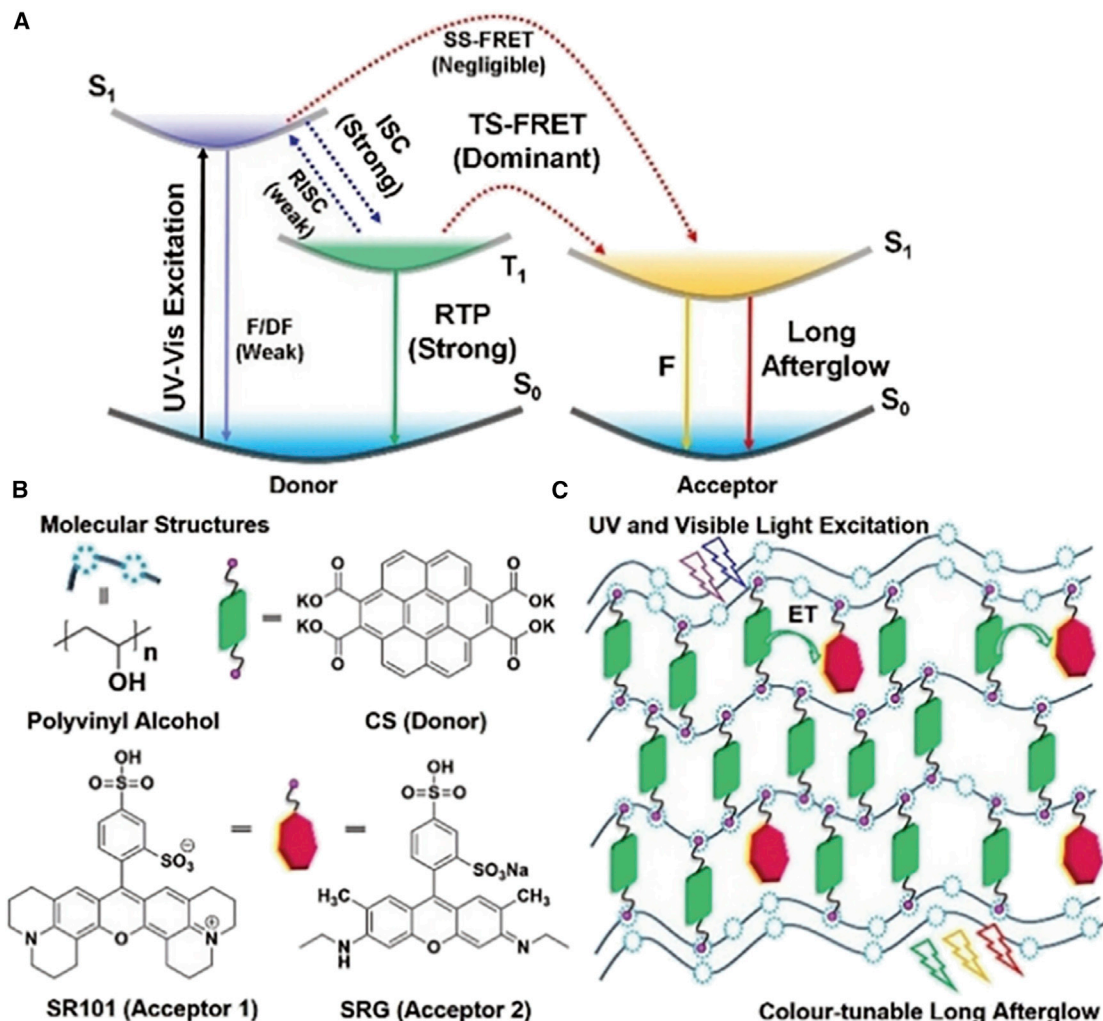


**Figure 12.** FRET induced multicolor RTP system

(A) Simplified Jablonski diagram to explain the phosphorescence energy transfer and other photophysical process in this case.

(B) Molecular structures of various components used in the study.

(C) Schematic representation of the PVA scaffold with anchored donor and acceptor chromophores to realize multicolor phosphorescence.<sup>99</sup> Reprinted from Kuila and George<sup>99</sup> with permissions from John Wiley & Sons (Copyright 2020).

to have the ability to suppress the vibration of the phosphors to generate RTP.<sup>102–105</sup> In this case, the polymers mainly serve as (1) a rigid structure and confinement environment provider, which inhibits the nonradiative transition pathway of doped small molecules; (2) a water and oxygen isolator to prevent the rapid annihilation of the generated triplet state; (3) polymers with heavy atoms or carbonyl structures can further improve ISC and the phosphorescence emission efficiency. In addition, polychromatic phosphorescent emission can be realized by simply replacing small molecules doped in the matrix. However, the way of introducing phosphors into the polymer system may be deferent, such as covalent linking, noncovalent binding, physical immobilization, or even direct generating RTP through the clusterization of the electron-rich atoms in the polymers.

#### Confining the phosphors by covalently linking into polymers

Because of thermal motions, collision, and exposure to quenchers, such as oxygen, it is difficult for pure small molecules to emit RTP. In contrast, these undesired

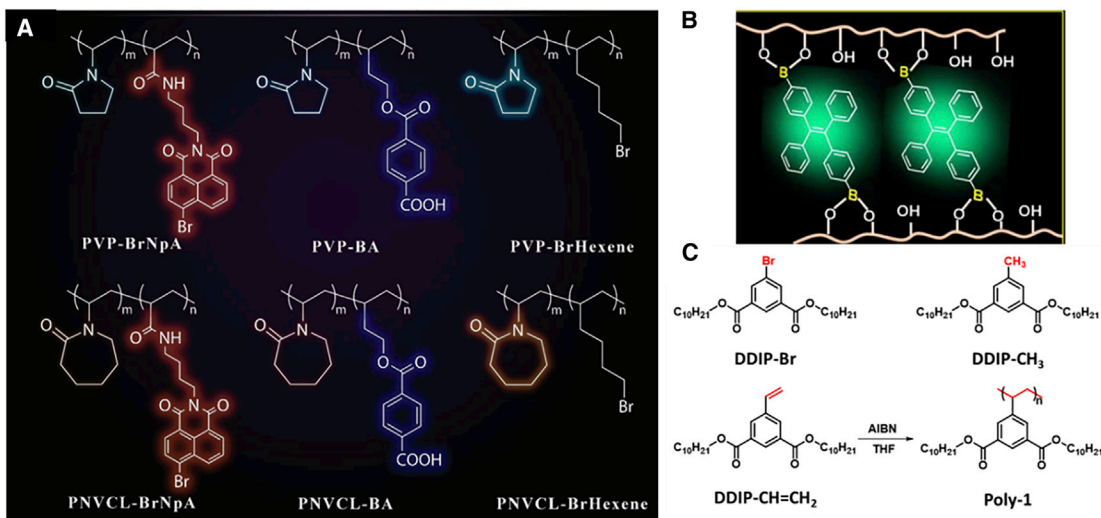


**Figure 13. Confining the phosphors by covalently linking into polymers**

(A) Molecular structures of PVP-BrNpA, PVP-BA, PVP-BrHexene, PNVCL-BrNpA, PNVCL-BA, and PNVCL-BrHexene.<sup>106</sup>

(B) Schematic representation for the polymer-based RTP using B-O click reaction.<sup>19</sup>

(C) Creation of RTP liquid crystals by covalently modifying small molecules with RTP to a polymer chain.<sup>107</sup>

Reprinted from Wang and co-workers<sup>106,107</sup> with permissions from John Wiley & Sons (Copyright 2019) and American Chemical Society (Copyright 2019).

processes can be avoided for polymers since the entanglement of the polymer chains may restrict the thermal motions and prevent the diffusion of quenchers to the internal. For this reason, scientists expected to connect the phosphorescent moieties onto the polymer chains to achieve RTP.

Amide functionalized polymers are the favorable choice to construct polymer-based RTP owing to the rigid environment provided by the polymer matrices and the hydrogen bonds. With this strategy, Ma and co-workers developed a series of pure organic phosphorescent polymers, such as PVP-BrNpA, PVP-BA, PVP-BrHexene, PNVCL-BrNpA, PNVCL-BA, and PNVCL-BrHexene, where N-vinylpyrrolidone (NVP) and N-vinylcaprolactam (NVCL) are employed as the dominant monomers to generate the polymer skeleton, while a small amount of other monomers, benzoic acid (BA), bromonaphthalimide (BrNpA), and 6-Br-1-hexene (BrHexene) are used as well.<sup>106</sup> The resultant RTP wavelength ranges from 422 to 582 nm, and the maximum phosphorescent quantum yield and lifetime are 1.6% and 0.95 ms, respectively (Figure 13A).

The low phosphorescent quantum yield can be enhanced by replacing the phosphorous moiety with the AIE ones. For instances, Lu and co-workers covalently immobilized the tetraphenylethylene-diboronic acid (TPEDB) into the polymer networks formed with PVA through the didiol reaction of PVA and borate (Figure 13B).<sup>19</sup> With increasing the content of boronic acid crosslinked TPEDB, the RTP intensity first rises and then falls. This is because the excessive TPEDB cannot be localized by PVA matrices, which results in energy dissipation through thermal motions. The DFT calculation further confirmed that the phosphorescence originated from the confined TPEDB by the PVA matrix.

If more than one luminescent group is copolymerized in the polymer, abundant luminescence can be detected. Huang and co-workers designed a multicomponent copolymer through radical crosslinked copolymerization of acrylic acid and multiple

luminophores.<sup>108</sup> By changing the excitation wavelength from 254 to 365 nm, these polymers display multicolor luminescence spanning from blue to yellow with a long-lived lifetime of 1.2 s and a maximum phosphorescence quantum yield of 37.5% under ambient conditions.

In addition to the usual amorphous powder-like RTP materials, polymerization is also an effective method to realize liquid crystal RTP materials. Though radical polymerization of DDIP-CH = CH<sub>2</sub>, Chen and co-workers successfully synthesized the first of the liquid crystal-type RTP materials, poly-1.<sup>107</sup> Poly-1 renders a columnar LC phase constructed by parallel packing of the supramolecular column, which is composed of two poly-1 chains (Figure 13C). In the column, the isophthalate phosphor is confined between the core of polymer backbones and the shell of decyl tails, and thus the nonradiative process is further suppressed.

#### Noncovalent interaction facilitated confinement of phosphors in polymers

In many cases, the phosphors may interact with the polymers through specific noncovalent interactions, which facilitate the confinement of the phosphors. The frequently employed noncovalent interactions include host-guest interaction, hydrogen bonding, and CT.

#### Host-guest interaction facilitated confinement of phosphors with polymers

Ma and co-workers achieved the cyan color RTP of anthracene by adding it into the  $\gamma$ -CD-modified polymer poly-AC (Figure 14A).<sup>109</sup> After photo irradiation, the anthracene undergoes [4 + 4] crosslinking to form dianthracene (An), which decreases the degree of conjugation. As a result, the RTP turned blue. Based on the same principle, Liu and co-workers obtained similar results by inclusion the polymer cationic side chain into CB (Figure 14B).<sup>110</sup>

#### Hydrogen bonding facilitated confinement of phosphors with polymers

Compared with host-guest interactions, hydrogen bonding between the polymer matrix and the phosphorous dopant is more convenient since there are many commercial polymers capable of forming hydrogen bonds. For instance, Yang and co-workers successfully achieved RTP by doping carefully selected organic chromophores into the PVA matrix through the hydrogen bonding and co-assembly strategy<sup>111</sup> (Figure 15A). In particular, when 3,6-diphenyl-9h-carbazole was chosen, the PVA films display a phosphorescent lifetime as long as 2044.86 ms and an afterglow duration of more than 20 s. Meanwhile, when doped with 7H-dibenzo[c,g]carbazole, a high absolute brightness of 158.4 mcd m<sup>2</sup> after removing the UV excitation source can be detected. According to the experimental and theoretical analysis, it is confirmed that the generation of this ultralong RTP is not only because of the rich hydrogen bonds that inhibit the nonradiative decay pathway, but also through narrowing the energy gap between the singlet and triplet states ( $\Delta E_{ST}$ ) by a co-assembly effect. Similar results are also obtained by others in the PVA matrix,<sup>112–114</sup> where planar dopants exhibit unexpected ultralong phosphorescence.

#### Electron-pulling effect facilitated confinement of phosphors with polymers

Although PVA may provide rich hydrogen bonds, which is helpful in inhibiting nonradiative transition and achieving long lifetime RTP, the luminescence in the system is extremely sensitive to water and humidity. Therefore, to develop RTP with excellent environmental tolerance via other noncovalent interactions is of practical importance. Tang and co-workers found that the electron-pulling effect is efficient in this regard.<sup>115</sup> By doping a series of small-molecular guests without RTP properties into the polyacrylonitrile (PAN), which is rich in electron-pulling cyano groups, they

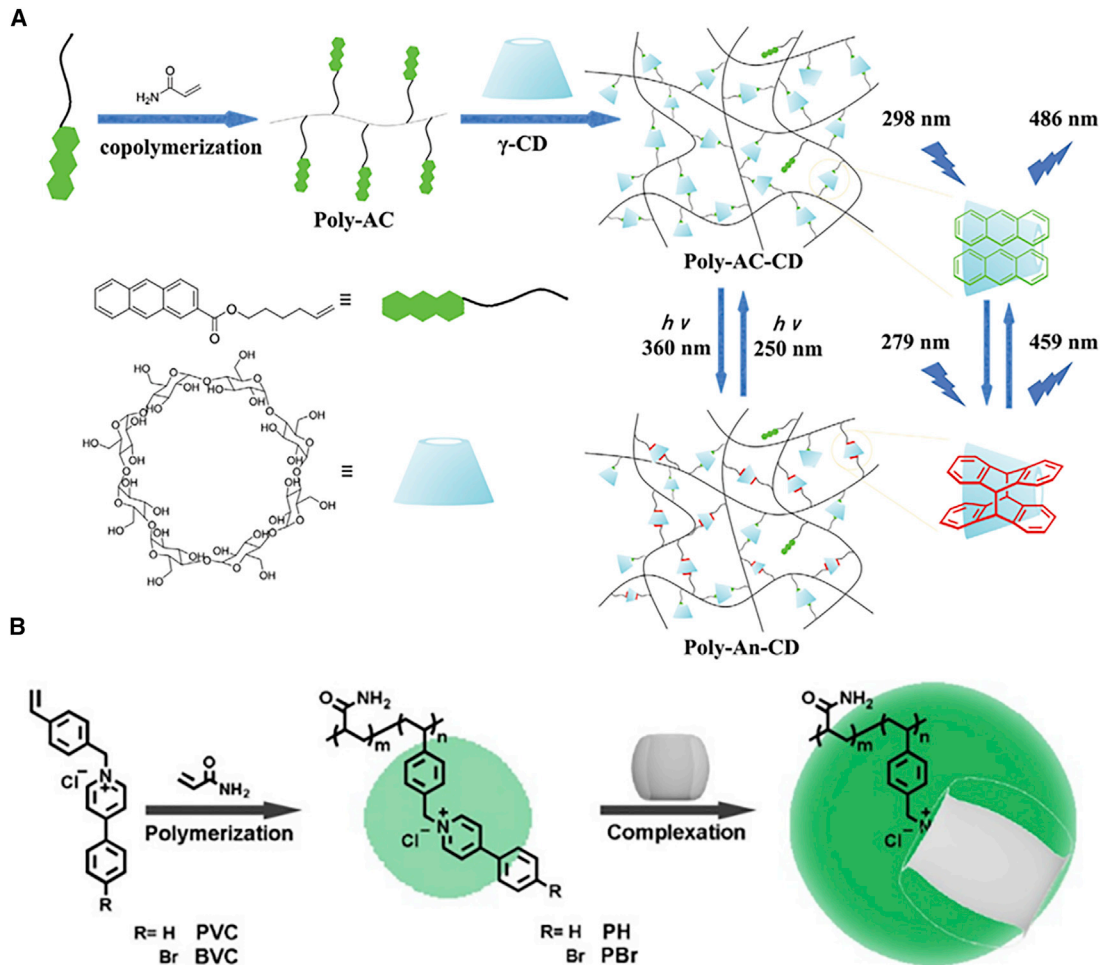


**Figure 14. Host-guest interaction facilitated confinement of phosphors with polymers**

(A) Illustration of luminous host-guest dynamic self-assembled pattern of anthracene polymers with  $\gamma$ -cyclodextrin, and the conversion to corresponding dimers by photocrosslinking reaction.<sup>109</sup>

(B) The synergistic enhancement (polymerization and complexation enhancement) strategy for ultralong and efficient room temperature phosphorescence.<sup>110</sup>

Reprinted from Lin and co-workers<sup>109,110</sup> with permissions from John Wiley & Sons (Copyright 2021 and 2020).

successfully obtained a series of amorphous phosphorescent PAN films (Figure 15B). In this attempt, the specific principle is that the electron-donating methoxy groups on the small-molecular guests TBB-6OMe, TPE-4OMe, NA-2OMe, and PY-OMe can enhance the ability of providing electrons, while the cyano groups in the PAN polymer has a strong electron-pulling tendency. Therefore, upon simple physical blending, a strong intermolecular electrostatic attraction is generated, which is capable of inhibiting the nonradiative transition path of triplet excitons and achieve considerable phosphorescence enhancement.

The photo stability of the dopants is also an important factor that determines the environmental tolerance of the RTP materials.<sup>114,117</sup> For this reason, Li and co-workers established a polymer-dopant system where PMMA is employed as the electron-pulling host and the photo stable phenothiazine derivatives as the guests<sup>116</sup> (Figure 15C). With the help of high emitting efficiency and the photo stability of the phenothiazine, these materials display an excellent photo stable RTP with a

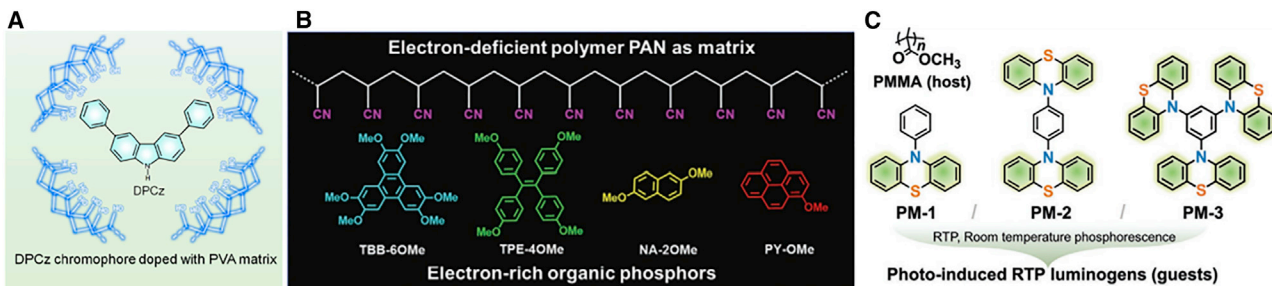


**Figure 15. Different intermolecular interaction facilitated RTP with polymers**

(A) Feasible strategy to achieve a long-lived RTP system by doping the heterocyclic polynuclear aromatic compound 3,6-diphenyl-9h-carbazole (DPCz) into the PVA matrix.<sup>111</sup>

(B) Chemical structures of polymer PAN and organic phosphors TBB-6OMe, TPE-4OMe, NA-2OMe, and PY-OMe.<sup>115</sup>

(C) The structures of phenothiazine derivatives and PMMA matrix.<sup>116</sup>

Reprinted from Zhang and co-workers<sup>111,115,116</sup> with permissions from American Chemical Society (Copyright 2021) and John Wiley & Sons (Copyright 2021 and 2020).

luminescence efficiency of over 22%, even at a low doping rate of 0.1%. When applied in afterglow imaging, a high-fidelity RTP image can be observed after repeated activation more than 50 times. This high brightness makes the material easy to be read even under outdoor daylight. Since the system is sensitive to oxygen, this light-induced RTP can also be used for leakage testing and nondestructive visual detection of microcracks in transparent media.

#### External heavy-atom effect facilitated RTP in polymer networks

The versatility of polymers renders more interactions with the dopants. Ionic polymers are composed of a polymeric backbone and counter ions. In the case of the counter ions being heavy atoms, the external heavy-atom effect may facilitate the generation of RTP for the dopants. Ma and co-workers reported an elegant example in this regard.<sup>47</sup> They employed the ionic polymer PAB, which has bromine counter ions. Upon doping cationic fluorescent dyes into the film of PAB, significant RTP is achieved. Replacing the bromine ions with the chloride ions would weaken the RTP, verifying that the external heavy atom contributes to this drastic RTP. Of course, the heavy atom facilitated triplet generation is stabilized by the rigid PAB network, since the bromine anion can form a rigid ion bond network with the quaternary amine cation on the main chain of the polymer, thus inhibiting the nonradiative pathway of the dye.

#### Charge separation facilitated rigidification of phosphors with polymers

It is also a very effective method to prolong the phosphorescence lifetime by charge separation between the polymeric host and the doped small-molecular guest. Adachi and co-workers achieved this goal using PBPO and tetramethylbenzidine (TMB) as a model<sup>118</sup> (Figure 16A). The result shows that the long persistent luminescence of 1 wt % TMB/PBPO in inert atmosphere at room temperature continues for more than 7 min after cutting off the excitation, which is significantly longer than traditional RTP (Figure 16B). The proposed mechanism is shown in Figure 16C. When the TMB/PBPO film is photoexcited under an inert atmosphere or vacuum conditions, singlet excited states are excited in TMB ( $S_{1,D}$ ). Since the CT interaction between TMB and PBPO is not efficient, the generated excitons are not fully converted into the exciplex singlet excited states ( $S_{1,E}$ ). Therefore, the remaining singlet excitons ( $S_{1,D}$ ) exhibit both fluorescence and RTP through ISC from  $S_{1,D}$  to the triplet excited state ( $T_{1,D}$ ). The generated exciplex singlet states can reversibly convert between the triplet ( $T_{1,E}$ ) and singlet states via ISC and reverse ISC because of the small energy gap

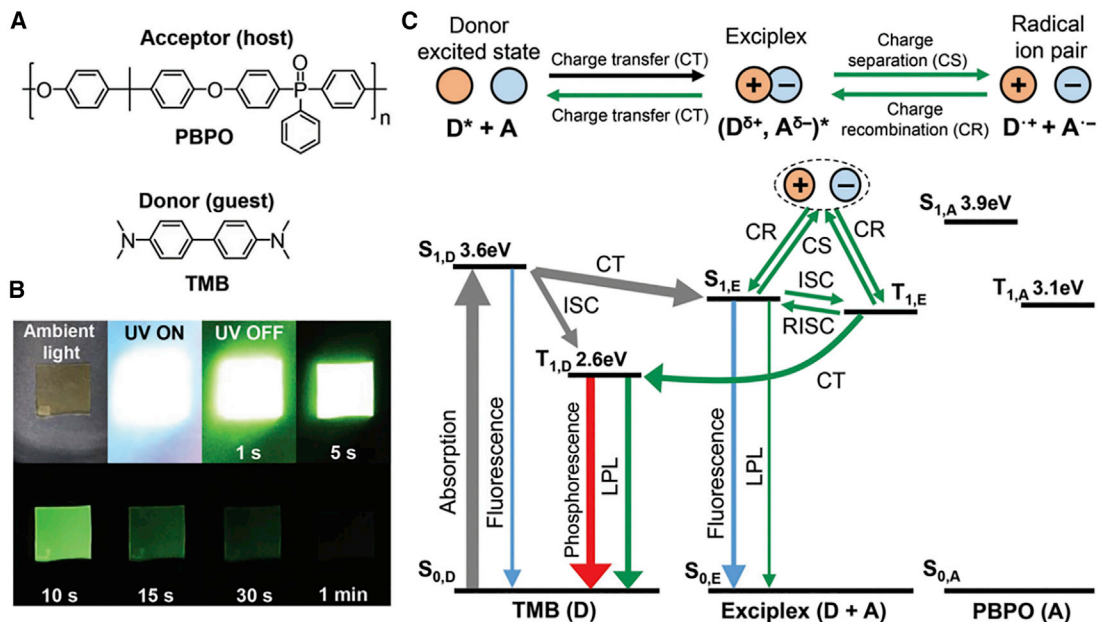


**Figure 16. Charge separation facilitated rigidification of phosphors with polymers**

(A) Molecular structure of PBPO and TMB.

(B) Photographs of a 1 wt % TMB/PBPO thick film at 298 K under the ambient light, during excitation by a 365 nm UV lamp, and at various times after turning off the excitation.

(C) Proposed mechanism for URTP.<sup>118</sup>

Reprinted from Lin et al.<sup>118</sup> with permissions from John Wiley & Sons (Copyright 2018).

between  $S_{1,E}$  and  $T_{1,E}$  at room temperature. However, the triplet exciplex ( $T_{1,E}$ ) does not produce delayed emission because the energy level of  $T_{1,D}$  is lower than that of  $T_{1,E}$ . In this combination of donor and acceptor,  $T_{1,E}$  is higher than  $T_{1,D}$  and  $T_{1,A}$ . Therefore, the triplet exciplex ( $T_{1,E}$ ) quickly transfers back to TMB ( $T_{1,D}$ ) through a CT process and emits light through phosphorescence from TMB.

#### Confinement of the phosphors by physically doping into polymer networks

The RTP generated by covalently linking the phosphorescent groups into the polymers requires considerable synthetic work. Considering that the role of the polymer is simply to immobilize the phosphorous groups, it is therefore envisioned that physical doping may also lead to RTP. Wang and co-workers verified this hypothesis by doping the organic phosphor TMB into the 3D polymer network formed with bisphenol-A and ethylenediamine.<sup>119</sup> A 2.28 s ultralong phosphorescence lifetime and up to 8.35% phosphorescence quantum yield is obtained upon the formation of the 3D network through copolymerization (Figure 17). This method has good universality. As tetrabenzylamine pyromellitate (TMP) is replaced by other molecules, such as, 4,4'-biphenol, N,N,N',N'-tetramethyl-1,4-phenylenediamine, TPA, and 2,6-diphenylphenol, RTP with lifetimes in the order of several hundreds of milliseconds are obtained. Furthermore, when the photochromic naphthopyran was used as the dopant, tunable fluorescent phosphorescent double emissions can be obtained upon controlling the density of crosslinking in the 3D network.<sup>120</sup>

#### RTP based on CTE

In addition to the introduction of traditional luminescent groups to realize ORTP, through-space conjugation (TSC) of electron-rich atoms, such as N, O, S, P, and Si, in a polymer system may also generate RTP. It has been recognized recently

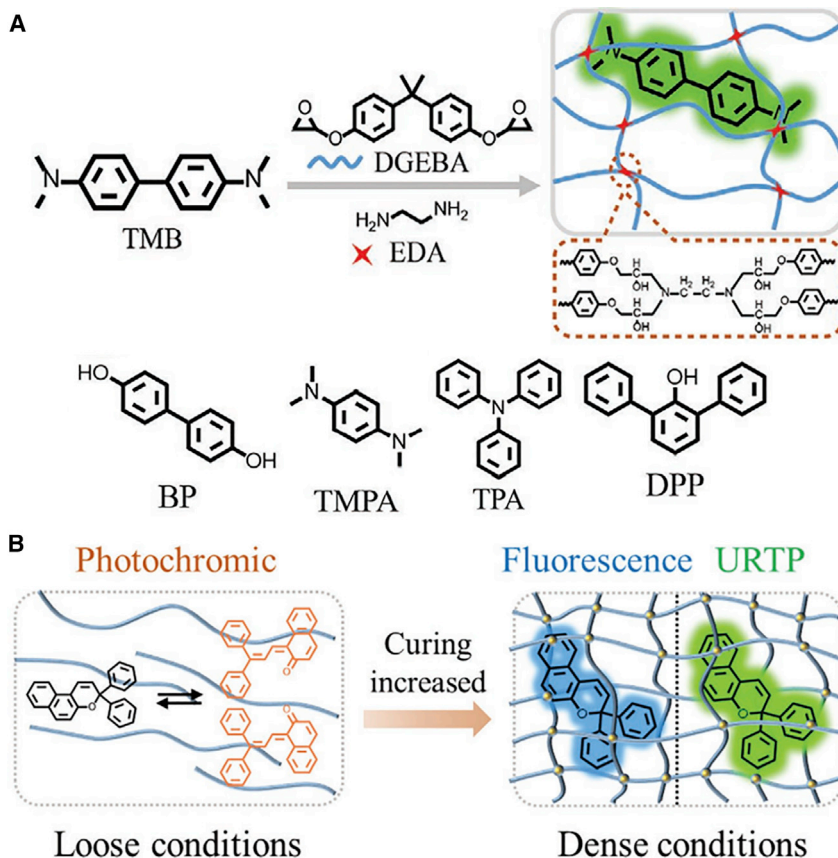


**Figure 17. Physically doping facilitated RTP**

(A) Molecular structure of TMB and polymer with its universality.<sup>119</sup>

(B) Molecular structure and the changing between photochromic properties and fluorescence-RTP dual emission.<sup>120</sup>

Reprinted from Wu and co-workers<sup>119,120</sup> with permissions from John Wiley & Sons (Copyright 2020 and 2021).

that many molecules without conjugated groups but with electron-rich atoms are able to give considerable emission.<sup>7,121,122</sup> Tang and co-workers revealed that, when the electron-rich atoms are clustered together, the extended delocalization of the lone pair electrons will occur by TSC, which results in conformation rigidification and CTE.<sup>123,124</sup> Most CTE is fluorescence, but CTE-based RTP is possible when the CTE state is dense enough to immobilize the TSC states. For instance, Yuan and co-workers found that some CTE materials are indeed able to give considerable phosphorescence.<sup>125,126</sup> Wei and co-workers reported that the commercially available noble metal and halogen-free polymer polyanetholesulfminic acid sodium salt alone is AIE active with blue-green phosphorescence of 0.5 ms.<sup>127</sup> Later, they found the commercial polymer poly(4-styrenesulfonic acid-co-maleic acid) salt also displays significant phosphorescence (Figure 18A).<sup>128</sup> Actually, RTP is now very common for a large variety of polymers. For instance, the nonionic polymer poly(ethylene terephthalate),<sup>129</sup>  $\epsilon$ -poly-L-lysine, sodium alginates (SA),<sup>130</sup> and many natural products, such as proteins and sugars,<sup>125,126</sup> are all found to give considerable RTP.

The presence of a simple aromatic ring, such as benzene or pyridine, may facilitate the CTE. An and co-workers synthesized a series of ultralong organic phosphorescent

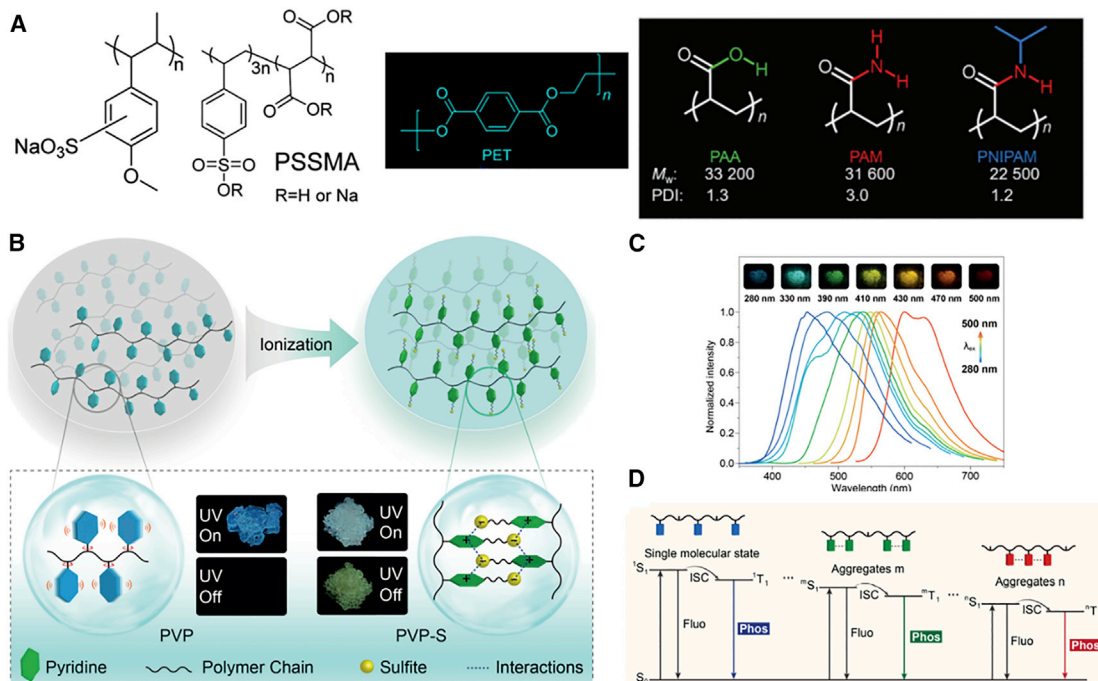


**Figure 18.** RTP based on clusterization-triggered emission

(A) Molecular structure formula of polymer with AIE-RTP.<sup>130</sup>

(B) Systematically illustration of ionization enabling ultralong organic phosphorescence in PVP polymers.

(C) Excitation-dependent phosphorescence spectra of PVP-S polymer at 77 K. Inset: photographs of afterglow for PVP-S polymer excited at 280, 330, 390, 410, 430, 470, and 500 nm at 77 K.

(D) Proposed mechanism of multicolor ultralong phosphorescence at different excitation wavelengths.<sup>131</sup>

Reprinted from Zhou and co-workers<sup>130,131</sup> with permissions from Royal Society of Chemistry (Copyright 2016) and John Wiley & Sons (Copyright 2019).

poly(4-vinylpyridine) (PVP) derivatives through a simple chemical ionization strategy<sup>131</sup> (Figures 18B–18D). After the ionization of 1,4-butanesulfonic acid lactone, the ultralong organic phosphorescent life of PVP-S can reach 578.36 ms, which is 525 times longer than PVP. Furthermore, they highlighted the adjustable phosphorescent color from blue to red under the stimulation of different excitation wavelengths. The different aggregation states of the side chain pyridine groups are responsible for this multicolor RTP. Similar study can also refer to other studies in their group, where the ionic bond crosslinking plays a key role in the phosphorescence enhancement and single-component multicolor emission of the traditional polystyrene derivatives.<sup>132</sup>

Although the CTE-type RTP have aroused ever-increasing attention, the variety of such polymers is still rare due to limited preparation strategies. Deng and co-workers successfully developed a CTE-RTP polymer through the hydrolyzation process of biobased nonconjugated polymers.<sup>133</sup> However, compared with the rich phosphorescent colors of other RTP materials, the CTE-RTPs are usually green, which greatly limits their application. The chemical modification of CTE molecules is an effective approach to enrich its phosphorescent emission color. In this regard, Yuan and co-workers obtained a series color-tunable RTP from blue to orange-red upon amidation grafting of luminophores onto SA.<sup>134</sup>

## Small molecules/ions facilitated RTP

Although suppressing the vibration of phosphors often requires a rigid host or networks formed by polymers, sometimes small molecules or ions can also induce RTP

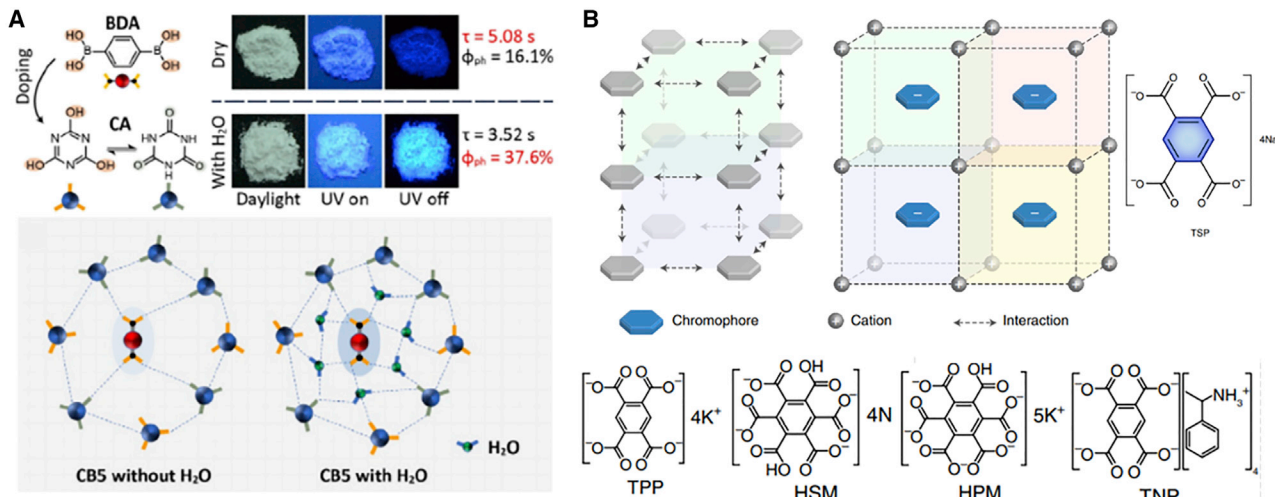


**Figure 19. Small molecules facilitate RTP**

(A) Molecular structure of BDA and CA with water facilitated phosphorescent materials and proposed mechanism.<sup>136</sup>

(B) Molecular structure of TSP, tetrapotassium pyromellitate (TPP), hexasodium mellitate (HSM), hexapotassium mellitate (HPM), and tetraammonium pyromellitate (TNP) and the cation rigidifying effect.<sup>137</sup>

Reprinted from Zhang and co-workers<sup>136,137</sup> with permissions from John Wiley & Sons (Copyright 2021) and Springer Nature (Copyright 2021).

for specific phosphors. In these cases, the phosphors may be rigidified by the small molecules/simple ions through formation of a network where the phosphor is part of the network. Although examples in this regard are not as judicious as previous demonstrations, it still deserves to be noted.

### Water facilitated RTP

It is well known that water is usually considered as a phosphorescence quencher due to the dissipation of the excitation energy through formation of hydrogen bonding with the phosphors.<sup>135</sup> However, water-induced phosphorescence quenching is true only when the water molecules are bonded individually. In a restricted space where the hydrogen bonding of water may form a network that can lock the phosphor, and water can stiffen the structure of the phosphor thus promoting RTP. For instance, Chen and co-workers developed an ultralong-life and deep-blue OURTP material by simply doping boron phosphor BDA into the cyanuric acid host using the stiffening effect of the water-hydrogen bond.<sup>136</sup> Merely the host-guest interaction between the two leads to RTP powders with an ultralong lifetime of 5.08 s and phosphorescence yield of 16.1%. In contrast, addition of water will build an extensive hydrogen bonding network between cyanuric acid and BDA, which further stiffens BDA. As a result, the phosphorescence yield increases from 16.1% to 37.6% (Figure 19A). We estimate the physical insight for the water enabled RTP observed by Liu and co-workers in Figure 2 is also the same with this example. This water-enhanced RTP makes it possible to use water as ink for luminescent writing.

### Simple ion-rendered repulsive forces enabled RTP

The fundamental physical insight for various RTP is the stiffening of the phosphors. Electrostatic repulsive forces are known to be able to stiffen flexible surfactant bilayers<sup>138,139</sup> and polyelectrolyte chains.<sup>140</sup> With the help of electrostatic repulsive forces, An and co-workers realized an ultralong RTP of up to 3 s with highly charged aromatic salts, including tetrapotassium pyromellitate, hexasodium mellitate, hexapotassium mellitate, tetraammonium pyromellitate, and TMP.<sup>137</sup> Because the aromatic salts are highly charged, they are stiffened by the electrostatic repulsive forces

between them, so that the RTP with the maximum phosphorescence yield of 96.5% can be achieved. Since the counter ions and the aromatic skeleton may influence the balance distance between the aromatic skeletons, larger counter ions and aromatic skeleton reduces the lifetime and the phosphorescence yield (Figure 19B). Since the smallest aromatic skeleton and the highest charge density facilitates optimal RTP, pure blue RTP can be generated in this way. This work inspires the design of high-efficiency blue organic phosphors and is expected to extend the domain of organic phosphorescence to new applications.

## CONCLUSIONS AND PERSPECTIVES

The common requirements of restricting the intramolecular movement for the generation of AIE and RTP have greatly decreased the difficulties for RTP. Since most AIE molecules that contain hybrid atoms can display phosphorescence, further suppressing the motion of all of the AIE molecules would facilely lead to RTP. It is envisioned that this molecular motion-suppressing strategy is also suitable for other fluorescent molecules, including those that usually display ACQ. The molecular motion suppression only requires a physical environment, which can be achieved by various noncovalent strategies. Different from the traditional strategies that highly depend on the covalent modification to obtain an ideal phosphor, diversified noncovalent protocols are enough to generate RTP from judicious fluorescent molecules. The major noncovalent protocols that may lead to RTP include host-guest interaction, hydrogen bonding, CT, electron pulling, electrostatic repulsive forces, and space confinement. With the suppression of the molecular motion of the phosphors, the long-lived triplet excitations would not dissipate through nonradiative inter- or intra-thermal motion of the phosphor. Specially, many co-crystal systems suppress the motion of the phosphors by rigidifying them through a CT process.

Solution or liquid-based RTP would become possible if the small-molecular phosphors can be restricted in a host. Macrocyclic hosts, such as CBs, that have extremely high binding constants with phosphorous guests are very intriguing in this regard. This makes it possible to clearly image the cancer cells without interference form the background biological fluorescence.

Polymers seem to be very promising as a medium to generate RTP, since all the polymers can form a network that is able to sufficiently confine the doped phosphors. The network formed by polymers can be further intensified by creation of a double network,<sup>141,142</sup> which is facilitated by the introduction of another polymer. Since the crosslinking density in the double network can be manipulated, it is even possible to generate RTP in hydrogels.

CTE could become an attractive origin of RTP, since it may offer green and economic phosphors without introducing any aromatic groups and heavy atoms. The clusterization of the hybrid atoms may create a superior dense network, which may even prevent the diffusion of quenchers, such as oxygen, into the internal. As a result, the RTP can be maintained under ambient conditions. Up to now, chemical modification is still the main method to regulate the phosphorescent color of CTE-RTP. Based on the understanding of intermolecular interactions, it may be hopeful in the future to realize more abundant luminescence of CTE and promote the CTE-RTP yield through noncovalent interactions.

Other elegant strategies that can lead to RTP are still upcoming and, with the formation of unexpected network structures, some unprecedented results can be

expected. We are optimistic in expecting the quenchers to turn into a helper that facilitates the generation of RTP, just as the role of water discussed in "water facilitated RTP" in this review. Furthermore, PRET would be very helpful in the field of RTP, since it allows us to generate luminescence with long lifetimes facilely by doping a classical fluorescent molecule to construct a pair of energy donors-acceptors. In addition, more complicated RTP phenomena, such as triplet-triplet annihilation,<sup>143,144</sup> TTET,<sup>145</sup> anti-kasha rule, two-photon phosphorescence,<sup>21</sup> are also undeveloped areas that deserve exploring.

## ACKNOWLEDGMENTS

This work is financially supported by the National Natural Science Foundation of China (NSFC 22172004 and 21972003).

## AUTHOR CONTRIBUTIONS

Discussion, J.H.; writing – original draft, T.W.; writing – review & editing, Y.Y.; supervision, Y.Y.

## DECLARATION OF INTERESTS

The authors declare no competing interests.

## REFERENCES

- Li, Y., Ma, B., Long, Y., Song, Z., Su, J., Wang, Y., Liu, R., Song, G., and Zhu, H. (2020). Aggregation-active phosphorescent emission-active Ir(iii) complexes with a long lifetime for specific mitochondrial imaging and tracking. *J. Mater. Chem. C* 8, 2467–2474.
- Lin, S., Pan, H., Li, L., Liao, R., Yu, S., Zhao, Q., Sun, H., and Huang, W. (2019). AIPE-active platinum(ii) complexes with tunable photophysical properties and their application in constructing thermosensitive probes used for intracellular temperature imaging. *J. Mater. Chem. C* 7, 7893–7899.
- Riebe, S., Vallet, C., van der Vight, F., Gonzalez-Abadelo, D., Wolper, C., Strassert, C.A., Jansen, G., Knauer, S., and Voskuhl, J. (2017). Aromatic thioethers as novel luminophores with aggregation-induced fluorescence and phosphorescence. *Chemistry* 23, 13660–13668.
- Guo, J., Li, X.-L., Nie, H., Luo, W., Gan, S., Hu, S., Hu, R., Qin, A., Zhao, Z., Su, S.-J., and Tang, B.Z. (2017). Achieving high-performance nondoped OLEDs with extremely small efficiency roll-off by combining aggregation-induced emission and thermally activated delayed fluorescence. *Adv. Funct. Mater.* 27, 1606458.
- He, Y., Fu, G., Li, W., Wang, B., Miao, T., Tan, M., Feng, W., and Lü, X. (2020). Efficient near-infrared (NIR) polymer light-emitting diode (PLED) based on the binuclear  $[(C^N)2Ir(bis-N^O)Ir(C^N)2]$  complex with aggregation-induced phosphorescent enhancement (AIPE) character. *J. Lumin.* 218, 116847.
- Yang, Z., Zhan, Y., Qiu, Z., Zeng, J., Guo, J., Hu, S., Zhao, Z., Li, X., Ji, S., Huo, Y., and Su, S.J. (2020). Stimuli-responsive aggregation-induced delayed fluorescence emitters featuring the asymmetric D-A structure with a novel diarylketone acceptor toward efficient OLEDs with negligible efficiency roll-off. *ACS Appl. Mater. Interfaces* 12, 29528–29539.
- Zheng, S., Zhu, T., Wang, Y., Yang, T., and Yuan, W.Z. (2020). Accessing tunable afterglows from highly twisted nonaromatic organic AIEGens via effective through-space conjugation. *Angew. Chem. Int. Ed. Engl.* 59, 10018–10022.
- Zhu, S., Hu, J., Zhai, S., Wang, Y., Xu, Z., Liu, R., and Zhu, H. (2020). AIPE-active Pt(ii) complexes with a tunable triplet excited state: design, mechanochromism and application in anti-counterfeiting. *Inorg. Chem. Front.* 7, 4677–4686.
- Jiang, K., Gao, X., Feng, X., Wang, Y., Li, Z., and Lin, H. (2020). Carbon dots with dual-emissive, robust, and aggregation-induced room-temperature phosphorescence characteristics. *Angew. Chem. Int. Ed. Engl.* 59, 1263–1269.
- Zhao, W., He, Z., and Tang, B.Z. (2020). Room-temperature phosphorescence from organic aggregates. *Nat. Rev. Mater.* 5, 869–885.
- Kenry, W., Chen, C., and Liu, B. (2019). Enhancing the performance of pure organic room-temperature phosphorescent luminophores. *Nat. Commun.* 10, 2111.
- Liu, H., Gao, Y., Cao, J., Li, T., Wen, Y., Ge, Y., Zhang, L., Pan, G., Zhou, T., and Yang, B. (2018). Efficient room-temperature phosphorescence based on a pure organic sulfur-containing heterocycle: folding-induced spin-orbit coupling enhancement. *Mater. Chem. Front.* 2, 1853–1858.
- Yu, J., Ma, H., Huang, W., Liang, Z., Zhou, K., Lv, A., Li, X.-G., and He, Z. (2021). Purely organic room-temperature phosphorescence endowing fast intersystem crossing from through-space spin-orbit coupling. *JACS Au* 1, 1694–1699.
- Yang, J., Fang, M., and Li, Z. (2021). Stimulus-responsive room temperature phosphorescence materials: internal mechanism, design strategy, and potential application. *Acc. Mater. Res.* 2, 644–654.
- Pan, S., Chen, Z., Zheng, X., Wu, D., Chen, G., Xu, J., Feng, H., and Qian, Z. (2018). Ultralong room-temperature phosphorescence from supramolecular behavior via intermolecular electronic coupling in pure organic crystals. *J. Phys. Chem. Lett.* 9, 3939–3945.
- Wu, H., Hang, C., Li, X., Yin, L., Zhu, M., Zhang, J., Zhou, Y., Agren, H., Zhang, Q., and Zhu, L. (2017). Molecular stacking dependent phosphorescence-fluorescence dual emission in a single luminophore for self-recoverable mechanoconversion of multicolor luminescence. *Chem. Commun.* 53, 2661–2664.
- Feng, H.T., Zeng, J., Yin, P.A., Wang, X.D., Peng, Q., Zhao, Z., Lam, J.W.Y., and Tang, B.Z. (2020). Tuning molecular emission of organic emitters from fluorescence to phosphorescence through push-pull electronic effects. *Nat. Commun.* 11, 2617.
- Yang, J., Zhang, Y., Wu, X., Dai, W., Chen, D., Shi, J., Tong, B., Peng, Q., Xie, H., Cai, Z., et al. (2021). Rational design of pyrrole derivatives with aggregation-induced phosphorescence characteristics for time-resolved and two-photon luminescence imaging. *Nat. Commun.* 12, 4883.
- Tian, R., Xu, S.M., Xu, Q., and Lu, C. (2020). Large-scale preparation for efficient polymer-based room-temperature phosphorescence via click chemistry. *Sci. Adv.* 6, eaaz6107.
- Mei, J., Leung, N.L., Kwok, R.T., Lam, J.W., and Tang, B.Z. (2015). Aggregation-induced emission: together we shine, united we soar! *Chem. Rev.* 115, 11718–11940.

21. Qin, W., Alifu, N., Lam, J.W.Y., Cui, Y., Su, H., Liang, G., Qian, J., and Tang, B.Z. (2020). Facile synthesis of efficient luminogens with AIE features for three-photon fluorescence imaging of the brain through the intact skull. *Adv. Mater.* 32, 2000364.
22. Li, Y., Tang, R., Liu, X., Gong, J., Zhao, Z., Sheng, Z., Zhang, J., Li, X., Niu, G., Kwok, R.T.K., et al. (2020). Bright aggregation-induced emission nanoparticles for two-photon imaging and localized compound therapy of cancers. *ACS Nano* 14, 16840–16853.
23. Zheng, Z., Li, D., Liu, Z., Peng, H.-Q., Sung, H.H.Y., Kwok, R.T.K., Williams, I.D., Lam, J.W.Y., Qian, J., and Tang, B.Z. (2019). Aggregation-induced nonlinear optical effects of AIegen nanocrystals for ultradeep *in vivo* bioimaging. *Adv. Mater.* 31, 1904799.
24. Luo, J., Xie, Z., Lam, J.W., Cheng, L., Chen, H., Qiu, C., Kwok, H.S., Zhan, X., Liu, Y., Zhu, D., and Tang, B.Z. (2001). Aggregation-induced emission of 1-methyl-1,2,3,4,5-pentaphenylsilole. *Chem. Commun.* 18, 1740–1741.
25. Yang, G., Li, S., Wang, S., and Li, Y. (2011). Emissive properties and aggregation-induced emission enhancement of excited-state intramolecular proton-transfer compounds. *C. R. Chim.* 14, 789–798.
26. Deol, H., Singh, G., Kumar, M., and Bhalla, V. (2019). Metal nanoparticles embedded in AIee active supramolecular assemblies: robust, green and reusable nanocatalysts. *Dalton Trans.* 48, 4769–4773.
27. Wang, H., Li, Y., Zhang, Y., Mei, J., and Su, J. (2019). A new strategy for achieving single-molecular white-light emission: using vibration-induced emission (VIE) plus aggregation-induced emission (AIE) mechanisms as a two-pronged approach. *Chem. Commun.* 55, 1879–1882.
28. Ramos-Soriano, J., Benitez-Benitez, S.J., Davis, A.P., and Galan, M.C. (2021). A vibration-induced-emission-based fluorescent chemosensor for the selective and visual recognition of glucose. *Angew. Chem. Int. Ed. Engl.* 60, 16880–16884.
29. Liu, P., Fu, W., Verwilt, P., Won, M., Shin, J., Cai, Z., Tong, B., Shi, J., Dong, Y., and Kim, J.S. (2020). MDM2-Associated clusterization-triggered emission and apoptosis induction effectuated by a theranostic spiropolymer. *Angew. Chem. Int. Ed. Engl.* 59, 8435–8439.
30. Zhang, H., Zhao, Z., McGonigal, P.R., Ye, R., Liu, S., Lam, J.W.Y., Kwok, R.T.K., Yuan, W.Z., Xie, J., Rogach, A.L., and Tang, B.Z. (2020). Clusterization-triggered emission: uncommon luminescence from common materials. *Mater. Today* 32, 275–292.
31. Liu, H., Guo, J., Zhao, Z., and Tang, B.Z. (2019). Aggregation-induced delayed fluorescence. *ChemPhotoChem* 3, 993–999.
32. Bai, H., Liu, Z., Zhang, T., Du, J., Zhou, C., He, W., Chau, J.H.C., Kwok, R.T.K., Lam, J.W.Y., and Tang, B.Z. (2020). Multifunctional supramolecular assemblies with aggregation-induced emission (AIE) for cell line identification, cell contamination evaluation, and cancer cell discrimination. *ACS Nano* 14, 7552–7563.
33. Qiu, Z.-J., Fan, S.-T., Xing, C.-Y., Song, M.-M., Nie, Z.-J., Xu, L., Zhang, S.-X., Wang, L., Zhang, S., and Li, B.-J. (2020). Facile fabrication of an AIE-active metal-organic framework for sensitive detection of explosives in liquid and solid phases. *ACS Appl. Mater. Interfaces* 12, 55299–55307.
34. Kong, R.-M., Zhang, X., Ding, L., Yang, D., and Qu, F. (2017). Label-free fluorescence turn-on aptasensor for prostate-specific antigen sensing based on aggregation-induced emission–silica nanospheres. *Anal. Bioanal. Chem.* 409, 5757–5765.
35. Zhang, D., Fan, Y., Chen, H., Trépout, S., and Li, M.-H. (2019). CO<sub>2</sub>-Activated reversible transition between polymersomes and micelles with AIE fluorescence. *Angew. Chem. Int. Ed. Engl.* 58, 10260–10265.
36. Yang, Y., Zhang, S., Zhang, X., Gao, L., Wei, Y., and Ji, Y. (2019). Detecting topology freezing transition temperature of vitrimers by AIE luminogens. *Nat. Commun.* 10, 3165.
37. Wu, B., Wu, H., Gong, Y., Li, A., Jia, X., and Zhu, L. (2021). A chiral single-component sol-gel platform with highly integrated optical properties. *J. Mater. Chem. C* 9, 4275–4280.
38. Wang, B., Liu, S., Liu, X., Hu, R., Qin, A., and Tang, B.Z. (2021). Aggregation-induced emission materials that aid in pharmaceutical research. *Adv. Healthc. Mater.* 10, 2101067.
39. Chen, Y.-Y., Jiang, X.-M., Gong, G.-F., Yao, H., Zhang, Y.-M., Wei, T.-B., and Lin, Q. (2021). Pillararene-based AIegens: research progress and appealing applications. *Chem. Commun.* 57, 284–301.
40. Han, X., Ge, F., Xu, J., and Bu, X.-H. (2021). Aggregation-induced emission materials for nonlinear optics. *Aggregate* 2, e28.
41. Hackney, H.E., and Perepichka, D.F. (2021). Recent advances in room temperature phosphorescence of crystalline boron containing organic compounds. *Aggregate*, e123. <https://doi.org/10.1002/agt2.123>.
42. Hou, Y., Jiang, G., Gong, J., Sha, R., and Wang, J. (2021). Recent advances of pure organic room temperature phosphorescence materials for bioimaging applications. *Chem. Res. Chin. Univ.* 37, 73–82.
43. Singh, M., Liu, K., Qu, S., Ma, H., Shi, H., An, Z., and Huang, W. (2021). Recent advances of cocrystals with room temperature phosphorescence. *Adv. Opt. Mater.* 9, 2002197.
44. Hirata, S., and Vacha, M. (2017). White afterglow room-temperature emission from an isolated single aromatic unit under ambient condition. *Adv. Opt. Mater.* 5, 1600996.
45. Ma, X.K., Zhang, W., Liu, Z., Zhang, H., Zhang, B., and Liu, Y. (2021). Supramolecular pins with ultralong efficient phosphorescence. *Adv. Mater.* 33, e2007476.
46. Wang, Z., Zheng, Y., Su, Y., Gao, L., Zhu, Y., Xia, J., Zhang, Y., Wang, C., Zheng, X., Zhao, Y., et al. (2021). Ultraviolet-activated long-lived room-temperature phosphorescence from small organic molecule-doped polymer systems. *Sci. China Mater.* <https://doi.org/10.1007/s40843-021-1768-6>.
47. Yan, Z.A., Lin, X., Sun, S., Ma, X., and Tian, H. (2021). Activating room-temperature phosphorescence of organic luminophores via external heavy-atom effect and rigidity of ionic polymer matrix\*. *Angew. Chem. Int. Ed. Engl.* 60, 19735–19739.
48. Giannini, C., Forni, A., Malpicci, D., Lucenti, E., Marinotto, D., Previtali, A., Carlucci, L., and Cariati, E. (2021). Room temperature phosphorescence from organic materials: unravelling the emissive behaviour of chloro-substituted derivatives of cyclic trimidazole. *Eur. J. Org. Chem.* 2021, 2041–2049.
49. Lucenti, E., Forni, A., Botta, C., Giannini, C., Malpicci, D., Marinotto, D., Previtali, A., Righetto, S., and Cariati, E. (2019). Intrinsic and extrinsic heavy-atom effects on the multifaceted emissive behavior of cyclic trimidazole. *Chemistry* 25, 2452–2456.
50. Zhang, J., Qiu, H., He, T., Li, Y., and Yin, S. (2020). Fluorescent supramolecular polymers formed by crown ether-based host-guest interaction. *Front. Chem.* 8, 560.
51. Ding, B., and Ma, X. (2021). A simple, easy preparation and tunable strategy for preparing organic room-temperature phosphorescence. *Langmuir* 37, 14229–14236.
52. Ma, X.K., and Liu, Y. (2021). Supramolecular purely organic room-temperature phosphorescence. *Acc. Chem. Res.* 54, 3403–3414.
53. Liu, G., Yuan, Q., Hollett, G., Zhao, W., Kang, Y., and Wu, J. (2018). Cyclodextrin-based host-guest supramolecular hydrogel and its application in biomedical fields. *Polym. Chem.* 9, 3436–3449.
54. Yan, Y., Jiang, L., and Huang, J. (2011). Unveil the potential function of CD in surfactant systems. *Phys. Chem. Chem. Phys.* 13, 9074–9082.
55. Liu, K., Ma, C., Wu, T., Qi, W., Yan, Y., and Huang, J. (2020). Recent advances in assemblies of cyclodextrins and amphiphiles: construction and regulation. *Curr. Opin. Colloid Interface Sci.* 45, 44–56.
56. Qi, W., Ma, C., Yan, Y., and Huang, J. (2021). Chirality manipulation of supramolecular self-assembly based on the host-guest chemistry of cyclodextrin. *Curr. Opin. Colloid Interface Sci.* 56, 101526.
57. Turro, N.J., Bolt, J.D., Kuroda, Y., and Tabushi, I. (1982). A study of the kinetics of inclusion of halonaphthalenes with β-cyclodextrin via time correlated phosphorescence. *Photochem. Photobiol.* 35, 69–72.
58. Huang, G., Deng, Z., Pang, J., Li, J., Ni, S., Li, J.A., Zhou, C., Li, H., Xu, B., Dang, L., and Li, M.D. (2021). Long-range charge transportation induced organic host-guest dual color long persistent luminescence. *Adv. Opt. Mater.* 9, 2101337.
59. Li, D., Lu, F., Wang, J., Hu, W., Cao, X.M., Ma, X., and Tian, H. (2018). Amorphous metal-free

- room-temperature phosphorescent small molecules with multicolor photoluminescence via a host-guest and dual-emission strategy. *J. Am. Chem. Soc.* 140, 1916–1923.
60. Shen, F.-F., Chen, Y., Dai, X., Zhang, H.-Y., Zhang, B., Liu, Y., and Liu, Y. (2021). Purely organic light-harvesting phosphorescence energy transfer by  $\beta$ -cyclodextrin pseudorotaxane for mitochondria targeted imaging. *Chem. Sci.* 12, 1851–1857.
61. Chen, P.Z., Chen, Y.Z., Tung, C.H., and Yang, Q.Z. (2018). A simple strategy to construct amorphous metal-free room temperature phosphorescent and multi-color materials. *ChemPhysChem* 19, 2131–2133.
62. Liu, H., Luan, Y., Koo, B., Lee, E.Y., Joo, J., Dao, T.N.T., Zhao, F., Zhong, L., Yun, K., and Shin, Y. (2019). Cucurbituril-based reusable nanocomposites for efficient molecular encapsulation. *ACS Sustain. Chem. Eng.* 7, 5440–5448.
63. Gu, L.-Q., Braha, O., Conlan, S., Cheley, S., and Bayley, H. (1999). Stochastic sensing of organic analytes by a pore-forming protein containing a molecular adapter. *Nature* 399, 686–690.
64. You, Y., Zhou, K., Guo, B., Liu, Q., Cao, Z., Liu, L., and Wu, H.-C. (2019). Measuring binding constants of cucurbituril-based host–guest interactions at the single-molecule level with nanopores. *ACS Sensors* 4, 774–779.
65. Mu, L., Yang, X.-B., Xue, S.-F., Zhu, Q.-J., Tao, Z., and Zeng, X. (2007). Cucurbit[n]uril-induced room temperature phosphorescence of quinoline derivatives. *Anal. Chim. Acta* 597, 90–96.
66. Zhang, Z.Y., Chen, Y., and Liu, Y. (2019). Efficient room-temperature phosphorescence of a solid-state supramolecule enhanced by cucurbit[6]uril. *Angew. Chem. Int. Ed. Engl.* 58, 6028–6032.
67. Zhang, Z.Y., and Liu, Y. (2019). Ultralong room-temperature phosphorescence of a solid-state supramolecule between phenylmethylpyridinium and cucurbit[6]uril. *Chem. Sci.* 10, 7773–7778.
68. Xu, L., Zou, L., Chen, H., and Ma, X. (2017). Room-temperature phosphorescence of cucurbit[7]uril recognized naphthalimide derivative. *Dyes Pigm.* 142, 300–305.
69. Wang, J., Huang, Z., Ma, X., and Tian, H. (2020). Visible-light-excited room-temperature phosphorescence in water by cucurbit[8]uril-mediated supramolecular assembly. *Angew. Chem. Int. Ed. Engl.* 59, 9928–9933.
70. Zhou, Y., Zhao, D., Li, Z.-Y., Liu, G., Feng, S.-H., Zhao, B.-T., and Ji, B.-M. (2021). Cucurbit[8]uril mediated ultralong purely organic phosphorescence and excellent mechanical strength performance in double-network supramolecular hydrogels. *Dyes Pigm.* 195, 109725.
71. Gong, Y., Chen, H., Ma, X., and Tian, H. (2016). A cucurbit[7]uril based molecular shuttle encoded by visible room-temperature phosphorescence. *ChemPhysChem* 17, 1934–1938.
72. Shen, F.-F., Chen, Y., Xu, X., Yu, H.-J., Wang, H., and Liu, Y. (2021). Supramolecular assembly with near-infrared emission for two-photon mitochondrial targeted imaging. *Small* 17, 2101185.
73. Yan, X., Peng, H., Xiang, Y., Wang, J., Yu, L., Tao, Y., Li, H., Huang, W., and Chen, R. (2021). Recent advances on host-guest material systems toward organic room temperature phosphorescence. *Small* 18, e2104073.
74. Notsuka, N., Kabe, R., Goushi, K., and Adachi, C. (2017). Confinement of long-lived triplet excitons in organic semiconducting host–guest systems. *Adv. Funct. Mater.* 27, 1703902.
75. Hirata, S., Totani, K., Zhang, J., Yamashita, T., Kaji, H., Marder, S.R., Watanabe, T., and Adachi, C. (2013). Efficient persistent room temperature phosphorescence in organic amorphous materials under ambient conditions. *Adv. Funct. Mater.* 23, 3386–3397.
76. Hirata, S., Totani, K., Kaji, H., Vacha, M., Watanabe, T., and Adachi, C. (2013). Reversible thermal recording media using time-dependent persistent room temperature phosphorescence. *Adv. Opt. Mater.* 1, 438–442.
77. Li, M., Cai, X., Chen, Z., Liu, K., Qiu, W., Xie, W., Wang, L., and Su, S.J. (2021). Boosting purely organic room-temperature phosphorescence performance through a host-guest strategy. *Chem. Sci.* 12, 13580–13587.
78. Lin, Z., Kabe, R., Wang, K., and Adachi, C. (2020). Influence of energy gap between charge-transfer and locally excited states on organic long persistence luminescence. *Nat. Commun.* 11, 191.
79. Yamanaka, T., Nakanotani, H., and Adachi, C. (2019). Slow recombination of spontaneously dissociated organic fluorophore excitons. *Nat. Commun.* 10, 5748.
80. Lei, Y., Dai, W., Tian, Y., Yang, J., Li, P., Shi, J., Tong, B., Cai, Z., and Dong, Y. (2019). Revealing insight into long-lived room-temperature phosphorescence of host-guest systems. *J. Phys. Chem. Lett.* 10, 6019–6025.
81. Wang, Y., Gao, H., Yang, J., Fang, M., Ding, D., Tang, B.Z., and Li, Z. (2021). High performance of simple organic phosphorescence host-guest materials and their application in time-resolved bioimaging. *Adv. Mater.* 33, e2007811.
82. Hernández, F.J., and Crespo-Otero, R. (2021). Excited state mechanisms in crystalline carbazole: the role of aggregation and isomeric defects. *J. Mater. Chem. C* 9, 11882–11892.
83. Chen, B., Huang, W., Su, H., Miao, H., Zhang, X., and Zhang, G. (2020). An unexpected chromophore-solvent reaction leads to bicomponent aggregation-induced phosphorescence. *Angew. Chem. Int. Ed. Engl.* 59, 10023–10026.
84. Chen, C., Chi, Z., Chong, K.C., Batsanov, A.S., Yang, Z., Mao, Z., Yang, Z., and Liu, B. (2021). Carbazole isomers induce ultralong organic phosphorescence. *Nat. Mater.* 20, 175–180.
85. Ding, B., Ma, L., Huang, Z., Ma, X., and Tian, H. (2021). Engendering persistent organic room temperature phosphorescence by trace ingredient incorporation. *Sci. Adv.* 7, eabf9668.
86. Chen, B., Huang, W., Nie, X., Liao, F., Miao, H., Zhang, X., and Zhang, G. (2021). An organic host-guest system producing room-temperature phosphorescence at the parts-per-billion level. *Angew. Chem. Int. Ed. Engl.* 60, 16970–16973.
87. Clapp, D.B. (1939). The phosphorescence of tetraphenylmethane and certain related substances. *J. Am. Chem. Soc.* 61, 523–524.
88. Bilen, C.S., Harrison, N., and Morantz, D.J. (1978). Unusual room temperature afterglow in some crystalline organic compounds. *Nature* 271, 235–237.
89. Ning, Y., Yang, J., Si, H., Wu, H., Zheng, X., Qin, A., and Tang, B.Z. (2021). Ultralong organic room-temperature phosphorescence of electron-donating and commercially available host and guest molecules through efficient Förster resonance energy transfer. *Sci. China Chem.* 64, 739–744.
90. Wang, Y., Yang, J., Fang, M., Yu, Y., Zou, B., Wang, L., Tian, Y., Cheng, J., Tang, B.Z., and Li, Z. (2020). Förster resonance energy transfer: an efficient way to develop stimulus-responsive room-temperature phosphorescence materials and their applications. *Matter* 3, 449–463.
91. Yang, J., Wu, X., Shi, J., Tong, B., Lei, Y., Cai, Z., and Dong, Y. (2021). Achieving efficient phosphorescence and mechanoluminescence in organic host-guest system by energy transfer. *Adv. Funct. Mater.* 31, 2108072.
92. Lei, Y., Yang, J., Dai, W., Lan, Y., Yang, J., Zheng, X., Shi, J., Tong, B., Cai, Z., and Dong, Y. (2021). Efficient and organic host-guest room-temperature phosphorescence: tunable triplet-singlet crossing and theoretical calculations for molecular packing. *Chem. Sci.* 12, 6518–6525.
93. Chen, Y., Xie, Y., Shen, H., Lei, Y., Zhou, Y., Dai, W., Cai, Z., Liu, M., Huang, X., and Wu, H. (2020). Tunable phosphorescence/fluorescence dual emissions of organic isoquinoline-benzophenone doped systems by alkoxy engineering. *Chemistry* 26, 17376–17380.
94. Zhang, X., Du, L., Zhao, W., Zhao, Z., Xiong, Y., He, X., Gao, P.F., Alam, P., Wang, C., Li, Z., et al. (2019). Ultralong UV/mechanical-excited room temperature phosphorescence from purely organic cluster excitons. *Nat. Commun.* 10, 5161.
95. Gao, R., and Yan, D. (2017). Layered host-guest long-afterglow ultrathin nanosheets: high-efficiency phosphorescence energy transfer at 2D confined interface. *Chem. Sci.* 8, 590–599.
96. Huo, M., Dai, X.Y., and Liu, Y. (2021). Ultrahigh supramolecular cascaded room-temperature phosphorescence capturing system. *Angew. Chem. Int. Ed. Engl.* 60, 27171–27177.
97. Xie, Z., Zhang, X., Wang, H., Huang, C., Sun, H., Dong, M., Ji, L., An, Z., Yu, T., and Huang, W. (2021). Wide-range lifetime-tunable and

- responsive ultralong organic phosphorescent multi-host/guest system. *Nat. Commun.* 12, 3522.
98. Wang, D., Xie, Y., Wu, X., Lei, Y., Zhou, Y., Cai, Z., Liu, M., Wu, H., Huang, X., and Dong, Y. (2021). Excitation-dependent triplet-singlet intensity from organic host-guest materials: tunable color, white-light emission, and room-temperature phosphorescence. *J. Phys. Chem. Lett.* 12, 1814–1821.
99. Kuila, S., and George, S.J. (2020). Phosphorescence energy transfer: ambient afterglow fluorescence from water-processable and purely organic dyes via delayed sensitization. *Angew. Chem. Int. Ed. Engl.* 59, 9393–9397.
100. Kuila, S., Garain, S., Bandi, S., and George, S.J. (2020). All-organic, temporally pure white afterglow in amorphous films using complementary blue and greenish-yellow ultralong room temperature phosphors. *Adv. Funct. Mater.* 30, 2003693.
101. Dang, Q., Jiang, Y., Wang, J., Wang, J., Zhang, Q., Zhang, M., Luo, S., Xie, Y., Pu, K., Li, Q., and Li, Z. (2020). Room-temperature phosphorescence resonance energy transfer for construction of near-infrared afterglow imaging agents. *Adv. Mater.* 32, e2006752.
102. Gan, N., Shi, H., An, Z., and Huang, W. (2018). Recent advances in polymer-based metal-free room-temperature phosphorescent materials. *Adv. Funct. Mater.* 28, 1802657.
103. Fang, M.-M., Yang, J., and Li, Z. (2019). Recent advances in purely organic room temperature phosphorescence polymer. *Chin. J. Polym. Sci.* 37, 383–393.
104. Wang, J., Lou, X.Y., Wang, Y., Tang, J., and Yang, Y.W. (2021). Recent advances of polymer-based pure organic room temperature phosphorescent materials. *Macromol. Rapid Commun.* 42, e2100021.
105. Gao, H., and Ma, X. (2021). Recent progress on pure organic room temperature phosphorescent polymers. *Aggregate* 2, e38.
106. Wang, D., Yan, Z., Shi, M., Dai, J., Chai, Q., Gui, H., Zhang, Y., and Ma, X. (2019). Employing lactam copolymerization strategy to effectively achieve pure organic room-temperature phosphorescence in amorphous state. *Adv. Opt. Mater.* 7, 1901277.
107. Zhang, Y.-F., Wang, Y.-C., Yu, X.-S., Zhao, Y., Ren, X.-K., Zhao, J.-F., Wang, J., Jiang, X.-Q., Chang, W.-Y., Zheng, J.-F., et al. (2019). Isophthalate-based room temperature phosphorescence: from small molecule to side-chain jacketed liquid crystalline polymer. *Macromolecules* 52, 2495–2503.
108. Gu, L., Wu, H., Ma, H., Ye, W., Jia, W., Wang, H., Chen, H., Zhang, N., Wang, D., Qian, C., et al. (2020). Color-tunable ultralong organic room temperature phosphorescence from a multicomponent copolymer. *Nat. Commun.* 11, 944.
109. Lin, X., Xu, Q., and Ma, X. (2021). Emission-tunable room-temperature phosphorescent polymers based on dynamic reversible supramolecule-mediated photocrosslinking. *Adv. Opt. Mater.* 10, 2101646.
110. Zhang, Z.Y., Xu, W.W., Xu, W.S., Niu, J., Sun, X.H., and Liu, Y. (2020). A synergistic enhancement strategy for realizing ultralong and efficient room-temperature phosphorescence. *Angew. Chem. Int. Ed. Engl.* 59, 18748–18754.
111. Zhang, Y., Su, Y., Wu, H., Wang, Z., Wang, C., Zheng, Y., Zheng, X., Gao, L., Zhou, Q., Yang, Y., et al. (2021). Large-area, flexible, transparent, and long-lived polymer-based phosphorescence films. *J. Am. Chem. Soc.* 143, 13675–13685.
112. Wu, H., Chi, W., Chen, Z., Liu, G., Gu, L., Bindra, A.K., Yang, G., Liu, X., and Zhao, Y. (2019). Achieving amorphous ultralong room temperature phosphorescence by coassembling planar small organic molecules with polyvinyl alcohol. *Adv. Funct. Mater.* 29, 1807243.
113. Su, Y., Zhang, Y., Wang, Z., Gao, W., Jia, P., Zhang, D., Yang, C., Li, Y., and Zhao, Y. (2020). Excitation-dependent long-life luminescent polymeric systems under ambient conditions. *Angew. Chem. Int. Ed. Engl.* 59, 9967–9971.
114. Zhang, Y., Gao, L., Zheng, X., Wang, Z., Yang, C., Tang, H., Qu, L., Li, Y., and Zhao, Y. (2021). Ultraviolet irradiation-responsive dynamic ultralong organic phosphorescence in polymeric systems. *Nat. Commun.* 12, 2297.
115. Wu, H., Wang, D., Zhao, Z., Wang, D., Xiong, Y., and Tang, B.Z. (2021). Tailoring noncovalent interactions to activate persistent room-temperature phosphorescence from doped polyacrylonitrile films. *Adv. Funct. Mater.* 31, 2101656.
116. Wang, Y., Yang, J., Fang, M., Gong, Y., Ren, J., Tu, L., Tang, B.Z., and Li, Z. (2021). New phenothiazine derivatives that exhibit photoinduced room-temperature phosphorescence. *Adv. Funct. Mater.* 31, 2101719.
117. Zang, L., Shao, W., Kwon, M.S., Zhang, Z., and Kim, J. (2020). Photoresponsive luminescence switching of metal-free organic phosphors doped polymer matrices. *Adv. Opt. Mater.* 8, 2000654.
118. Lin, Z., Kabe, R., Nishimura, N., Jinnai, K., and Adachi, C. (2018). Organic long-persistent luminescence from a flexible and transparent doped polymer. *Adv. Mater.* 30, e1803713.
119. Wu, B., Guo, N., Xu, X., Xing, Y., Shi, K., Fang, W., and Wang, G. (2020). Ultralong and high-efficiency room temperature phosphorescence of organic-phosphors-doped polymer films enhanced by 3D network. *Adv. Opt. Mater.* 8, 2001192.
120. Wu, B., Xu, X., Tang, Y., Han, X., and Wang, G. (2021). Multifunctional optical polymeric films with photochromic, fluorescent, and ultra-long room temperature phosphorescent properties. *Adv. Opt. Mater.* 9, 2101266.
121. Liao, P., Zang, S., Wu, T., Jin, H., Wang, W., Huang, J., Tang, B.Z., and Yan, Y. (2021). Generating circularly polarized luminescence from clusterization-triggered emission using solid phase molecular self-assembly. *Nat. Commun.* 12, 5496.
122. Liao, P., Huang, J., Yan, Y., and Tang, B.Z. (2021). Clusterization-triggered emission (CTE): one for all, all for one. *Mater. Chem. Front.* 5, 6693–6717.
123. Zhou, Q., Cao, B., Zhu, C., Xu, S., Gong, Y., Yuan, W.Z., and Zhang, Y. (2016). Clusterization-triggered emission of nonconjugated polyacrylonitrile. *Small* 12, 6586–6592.
124. Wang, Y., Bin, X., Chen, X., Zheng, S., Zhang, Y., and Yuan, W.Z. (2018). Emission and emissive mechanism of nonaromatic oxygen clusters. *Macromol. Rapid Commun.* 39, e1800528.
125. Zheng, S., Hu, T., Bin, X., Wang, Y., Yi, Y., Zhang, Y., and Yuan, W.Z. (2020). Clusterization-triggered efficient room-temperature phosphorescence from nonconventional luminophores. *ChemPhysChem* 21, 36–42.
126. Wang, Q., Dou, X., Chen, X., Zhao, Z., Wang, S., Wang, Y., Sui, K., Tan, Y., Gong, Y., Zhang, Y., and Yuan, W.Z. (2019). Reevaluating protein photoluminescence: remarkable visible luminescence upon concentration and insight into the emission mechanism. *Angew. Chem. Int. Ed. Engl.* 58, 12667–12673.
127. Qin, X., Wang, S., Luo, L., He, G., Sun, H., Gong, Y., Jiang, B., and Wei, C. (2018). AIE-active polyanetholesulfonic acid sodium salts with room-temperature phosphorescence characteristics for Fe<sup>3+</sup> detection. *RSC Adv.* 8, 31231–31236.
128. Zou, L., Qin, X., Sun, H., Wang, S., Ding, W., Liu, Y., Wei, C., Jiang, B., and Gong, Y. (2019). Room-temperature phosphorescent polymers with excitation-wavelength and delay-time emission dependencies. *RSC Adv.* 9, 36287–36292.
129. Chen, X., He, Z., Kausar, F., Chen, G., Zhang, Y., and Yuan, W.Z. (2018). Aggregation-induced dual emission and unusual luminescence beyond excimer emission of poly(ethylene terephthalate). *Macromolecules* 51, 9035–9042.
130. Zhou, Q., Wang, Z., Dou, X., Wang, Y., Liu, S., Zhang, Y., and Yuan, W.Z. (2019). Emission mechanism understanding and tunable persistent room temperature phosphorescence of amorphous nonaromatic polymers. *Mater. Chem. Front.* 3, 257–264.
131. Wang, H., Shi, H., Ye, W., Yao, X., Wang, Q., Dong, C., Jia, W., Ma, H., Cai, S., Huang, K., et al. (2019). Amorphous ionic polymers with color-tunable ultralong organic phosphorescence. *Angew. Chem. Int. Ed. Engl.* 58, 18776–18782.
132. Cai, S., Ma, H., Shi, H., Wang, H., Wang, X., Xiao, L., Ye, W., Huang, K., Cao, X., Gan, N., et al. (2019). Enabling long-lived organic room temperature phosphorescence in polymers by subunit interlocking. *Nat. Commun.* 10, 4247.
133. Zhao, B., Yang, S., Yong, X., and Deng, J. (2021). Hydrolyzation-triggered ultralong room-temperature phosphorescence in biobased nonconjugated polymers. *ACS Appl. Mater. Interfaces* 13, 59320–59328.
134. Dou, X., Zhu, T., Wang, Z., Sun, W., Lai, Y., Sui, K., Tan, Y., Zhang, Y., and Yuan, W.Z. (2020). Color-tunable, excitation-dependent, and time-dependent afterglows from pure

- organic amorphous polymers. *Adv. Mater.* 32, e2004768.
135. Gao, H., Ding, B., Wang, C., and Ma, X. (2021). Synergetic enhancement of room-temperature phosphorescence via water molecules as a hydrogen bonding bridge. *J. Mater. Chem. C* 9, 16581–16586.
136. Zhang, J., Xu, S., Wang, Z., Xue, P., Wang, W., Zhang, L., Shi, Y., Huang, W., and Chen, R. (2021). Stimuli-responsive deep-blue organic ultralong phosphorescence with lifetime over 5 s for reversible water-jet anti-counterfeiting printing. *Angew. Chem. Int. Ed. Engl.* 60, 17094–17101.
137. Ye, W., Ma, H., Shi, H., Wang, H., Lv, A., Bian, L., Zhang, M., Ma, C., Ling, K., Gu, M., et al. (2021). Confining isolated chromophores for highly efficient blue phosphorescence. *Nat. Mater.* 20, 1539–1544.
138. Yan, Y., Li, L., and Hoffmann, H. (2006). Clouding: origin of phase separation in oppositely charged polyelectrolyte/surfactant mixed solutions. *J. Phys. Chem. B* 110, 1949–1954.
139. Yan, Y., Hoffmann, H., Drechsler, M., Talmon, Y., and Makarsky, E. (2006). Influence of hydrocarbon surfactant on the aggregation behavior of silicone surfactant: observation of intermediate structures in the Vesicle–Micelle transition. *J. Phys. Chem. B* 110, 5621–5626.
140. Cao, Y., Fang, Y., Nishinari, K., and Phillips, G.O. (2016). Effects of conformational ordering on protein/polyelectrolyte electrostatic complexation: ionic binding and chain stiffening. *Sci. Rep.* 6, 23739.
141. Xu, X., Jerca, V.V., and Hoogenboom, R. (2021). Bioinspired double network hydrogels: from covalent double network hydrogels via hybrid double network hydrogels to physical double network hydrogels. *Mater. Horiz.* 8, 1173–1188.
142. Huang, Y., Zhou, J., Sun, P., Zhang, L., Qian, X., Jiang, S., and Shi, C. (2021). Green, tough and highly efficient flame-retardant rigid polyurethane foam enabled by double network hydrogel coatings. *Soft Matter* 17, 10555–10565.
143. Chen, K., Hussain, M., Razi, S.S., Hou, Y., Yildiz, E.A., Zhao, J., Yaglioglu, H.G., and Donato, M.D. (2020). Anthryl-appended platinum(II) schiff base complexes: exceptionally small stokes shift, triplet excited states equilibrium, and application in triplet-triplet-annihilation upconversion. *Inorg. Chem.* 59, 14731–14745.
144. Wan, S., Lin, J., Su, H., Dai, J., and Lu, W. (2018). Photochemically deoxygenating solvents for triplet-triplet annihilation photon upconversion operating in air. *Chem. Commun.* 54, 3907–3910.
145. Zhao, W., Cheung, T.S., Jiang, N., Huang, W., Lam, J.W.Y., Zhang, X., He, Z., and Tang, B.Z. (2019). Boosting the efficiency of organic persistent room-temperature phosphorescence by intramolecular triplet-triplet energy transfer. *Nat. Commun.* 10, 1595.